

Proton Conductive Polymer/Metal Organic Framework Composite Membranes

A THESIS

SUBMITTED TO THE DEPARTMENT OF ADVANCED MATERIALS
AND NANOTECHNOLOGY AT THE GRADUATE SCHOOL OF
NATURAL SCIENCES OF ABDULLAH GUL UNIVERSITY
IN PARTIAL FULFILLMENT OF THE REQUIREMENTS
FOR THE DEGREE OF
MASTER OF SCIENCE

By

Mustafa ERKARTAL

July, 2015

Mustafa
ERKARTAL
Proton Conductive Polymer/Metal Organic Framework Composite
Membranes

AGU
2015

Proton Conductive Polymer/Metal Organic Framework Composite Membranes

A THESIS

SUBMITTED TO THE DEPARTMENT OF ADVANCED MATERIALS AND
NANOTECHNOLOGY AT THE GRADUATE SCHOOL OF NATURAL SCIENCES
OF ABDULLAH GUL UNIVERSITY

IN PARTIAL FULFILLMENT OF THE REQUIREMENTS

FOR THE DEGREE OF
MASTER OF SCIENCE

By

Mustafa Erkartal

July 2015

I certify that I have read this thesis and that in my opinion it is fully adequate, in scope and in quality, as a thesis for the degree of Master of Science.

Assoc. Prof. Dr. Ünal ŞEN
Supervisor

I certify that I have read this thesis and that in my opinion it is fully adequate, in scope and in quality, as a thesis for the degree of Master of Science.

(Assoc. Prof. Dr. Hakan USTA)

I certify that I have read this thesis and that in my opinion it is fully adequate, in scope and in quality, as a thesis for the degree of Master of Science.

(Assoc. Prof. Dr. Halil ŞAHAN)

Approved for the Graduate School of Natural Sciences:

Prof. Dr. İrfan Alan
Director of Graduate School of Natural Sciences

ABSTRACT

**PROTON CONDUCTIVE POLYMER/METAL ORGANIC
FRAMEWORK COMPOSITE MEMBRANES**

Mustafa Erkartal

MSc. in Advanced Materials and Nanotechnology

Supervisor: Assoc. Prof. Dr. Ünal Şen

July, 2015

Proton exchange membrane fuel cells (PEMFCs) are one of the most innovative research areas in search of novel power sources, especially because of their no to low greenhouse gas emissions, high efficiency, diverse fuel options and low maintenance costs. Hence, PEMFCs are regarded as one of the potential alternatives for the conventional power generators. Proton exchange membrane (PEM) is the core component of the PEMFC. Still, Nafion® and PBI are the commonly used membrane materials in fuel cell technology. The development of novel PEMs with high proton conductivity, good mechanical and chemical stability and cost-effective manufacturing remain as obstacles for the commercialization of PEMFCs. In this thesis for the first time, we present preparation and characterization of two types of novel composite proton exchange membranes which consist of zeolitic imidazolat framework-8 (ZIF-8). In the first part of this study, consisting of poly(vinyl alcohol) (PVA), poly(2-acrylamido-2-methyl-1-propanesulfonic acid) (PAMPS) and zeolitic imidazolat framework-8 (ZIF-8) ternary Nafion-like composite membranes were prepared with different composition to use in the PEMFCs which of their operation temperatures below 100 °C. All of the membranes were structurally characterized and their proton conductivities were measured by electrochemical impedance spectroscopy. The fully hydrated membrane with 55 PVA/40 PAMPS/5 ZIF-8 composition shows the highest proton conductivity with about 0.13 S cm⁻¹ at 80 °C and the result thus obtained is comparable to the proton conductivity value of the Nafion in the literature. The aim of second part of this study is the preparing of membranes for high temperature proton exchange fuel cells (HTPEMFCs), which operate between 100-200 °C, the binary mixed membrane were manufactured incorporation of PBI and ZIF-8. In the membrane PBI

was used as host polymer whereas ZIF-8 is used as filler material. Among the structurally well-characterized membranes, the membrane with 12.5 ZIF-8/PBI membrane has the highest proton conductivity with about 0.0045 S cm^{-1} at $160 \text{ }^{\circ}\text{C}$ under anhydrous condition.

Keywords: Proton exchange membrane fuel cells, PAMPS, PVA, PBI, ZIF-8,

ÖZET

PROTON İLETKEN POLİMER/METAL ORGANİK KAFES YAPILAR İÇEREN KOMPOZİT MEMBRANLAR

Mustafa Erkartal

İleri Malzemeler ve Nanoteknoloji Anabilim Dalı Yüksek Lisans

Tez Yöneticisi: Doç. Dr. Ünal Şen

Temmuz ,2015

Proton değişim membranlı yakıt hücreleri (PDMYH), düşük sera gazı emisyonları, yüksek verimlilikleri, farklı yakıt seçenekleri ve düşük bakım maliyetleri nedeniyle yeni enerji kaynağı arayışında üzerine en çok çalışma yapılan alanlardan biridir. Bu yüzden, PDMYH'leri geleneksel güç üreticilerinin yerine geçebilecek en potansiyel aday konumundadır. Proton değişimli membran (PDM) bir yakıt hücresinin en temel parçasıdır. Halihazırda Nafion® ve PBI yakıt hücrelerinde sıklıkla kullanılan malzemelerdir. Yüksek proton iletkenliğine sahip, iyi kimyasal ve mekanik kararlılığa sahip, üretim maliyetleri düşük olan yeni PDM'lerin üretilmemesi PDMYH'lerin ticarileşmesinin önündeki en büyük engellerden biridir. Bu tezde ilk defa, zeolitik imidazol çerçeve yapıları (ZIF) içeren iki tür yeni proton değişimli kompozit membranlar üretildi. Çalışmanın ilk bölümünde, polivinil alkol (PVA), poli-2-akrilamit-2-metil propan sülfonik asit (PAMPS) ve ZIF-8'den oluşan, 3 bileşenli kompozit membranlar, çalışma sıcaklığı 100 °C altında olan yakıt hücreleri için üretildi. Nafion'un kimyasal yapısına benzetilerek üretilen bu membranların yapısal analizleri yapıldı ve proton iletkenlikleri elektrokimyasal impedans spektroskopisi ile yapıldı. Bu membranlardan ağırlıkça 55 PVA/40 PAMPS/5 ZIF-8 kompozisyona sahip olan membran, %100 nemli olarak 80°C'de 0.13 S cm⁻¹ büyüklüğünde bir proton iletkenlik değerine sahiptir. Bu değer literatürde yer alan, aynı koşullarda Nafion®'nun sahip olduğu iletkenlik değerinden yüksektir. Bu çalışmanın ikinci bölümünde ise, çalışma sıcaklık aralığı 100-200 °C aralığında olan yüksek sıcaklık proton değişim membranlı yakıt hücresinde kullanılabilecek kompozit membranlar üretilmiştir. Bu kompozit membranlar matris malzeme olarak polibenzimidazol (PBI) kullanılırken, ZIF-8 nano parçacıkları ise takviye malzemesi olarak kullanılmıştır. Farklı kompozisyonlarda

retilen bu membranlarda ise ađırlıka 12.5 ZIF-8/PBI kompozisyona sahip olan membran nemsiz ortamda, 160 °C' de 0.0045 S cm⁻¹ proton iletkenlik deđerine sahiptir. Bu deđer PBI'ın aynı kořullar altında llen iletkenliđi ile karřılařtırılabilir bir deđerdir.

Anahtar kelimeler: Proton deđiřim membranlı yakıt hcreleri, PVA, PAMPS, PBI, ZIF-8

Acknowledgements

Foremost, I'd like to offer my deepest appreciation to my supervisor Assoc. Professor Ünal Şen for his patience and guidance throughout this research project in the new and exciting field of fuel cells and metal organic frameworks. His guidance helped me in all the time of research and writing of this thesis. I could not have imagined having a better advisor and mentor for my PhD study.

And secondly, I thank to Assoc Professor Hakan Usta for his helpful insight on several occasions. Also, the polymer class that he taught touched on important aspects of this research project.

I thank my fellow labmates in Abdullah Gül University Duygu Tahaoglu, Mehmet Özdemir and Şeyma Dadı for the interesting discussions and the sleepless mornings we were working together before deadlines, and for all the fun we have had in the last two years.

And also I thank my friends: Hüseyin Çilsalar for being always right, (Master) Sinan Genç for his problem-solving skills about every aspects of life, Oğuzhan Ayyildiz for our pleasurable conversations about everything from science to relationship, Abdullah Oran for his meaningless glances when asked a question, Hatice Taş for her delicious handmade cakes, chocolates and coffee, Cengiz Gazeloglu to enlighten us about the magic world of statistics and Menderes Ülker to color our office life with his sympathetic behaviors.

I also would like acknowledge AGU and AGU BAP to fund my thesis. This study was supported by AGU BAP Project No: FYL-2014-7.

Last but not the least, I would like to thank my family: my parents Şaban and Cemile, for giving birth to me and supporting me spiritually throughout my life, and brother Murat and sister Merve for their endless supports and love.

And finally, as Mark Twain said that “What would men be without women? Scarce, sir...mighty scarce.” What would I do without you! I thank you my love, Ayşe, for being in my life.

Table of Contents

1. INTRODUCTION	1
2. INTRODUCTION TO FUEL CELLS	5
2.1 WHAT IS A FUEL CELL?	5
2.2 TYPES OF FUEL CELLS	7
2.3 PROTON EXCHANGE MEMBRANE FUEL CELL	8
2.3 MAIN FUEL CELL COMPONENTS AND MATERIALS	10
2.3.1 Catalyst Layer	10
2.3.2 Gas Diffusion Layer	12
2.3.3 Membrane	12
2.4 PROTON TRANSFER MECHANISM	14
2.4.1 Grotthuss-Type Mechanism	14
2.4.2 Vehicle-Type Mechanism	15
3. PROTON CONDUCTING NAFION-LIKE TERNARY PVA/PAMPS/ZIF-8 COMPOSITE MEMBRANES	16
3.1 LITERATURE SURVEY	16
3.2 EXPERIMENTAL	18
3.2.1 Materials	18
3.2.2 Synthesis of ZIF-8 nanoparticles	18
3.2.3 Membrane Preparation	19
3.3 CHARACTERIZATION	20
3.3.1 X-Ray Diffraction (XRD)	20
3.3.2 Fourier Transform Infrared Spectroscopy (FT-IR)	21
3.3.3 Thermo-gravimetric Analysis (TGA)	21
3.3.4 Scanning Electron Microscopy (SEM)	21
3.3.5 Proton Conductivity	21
3.3.6 Water Uptake (WU)	21
3.3.7 Ion Exchange Capacity (IEC)	22
3.4 RESULTS AND DISCUSSIONS	22
3.4.1 X-Ray Diffraction (XRD)	22
3.4.2 Fourier Transform Infrared Spectroscopy (FT-IR)	25
3.4.3 Thermo-Gravimetric Analysis (TGA)	26
3.4.4 Scanning Electron Microscopy	28
3.4.5 Water Uptake (WU) and Ion Exchange Capacity (IEC)	30
3.4.6 Proton Conductivity	33
3.5 CONCLUSIONS	34
4. PROTON CONDUCTING ZIF-8/PBI MIXED MATRIX MEMBRANES FOR HIGH TEMPERATURES PROTON EXCHANGE MEMBRANES FUEL CELLS	36
4.1 LITERATURE SURVEY	36
4.2 EXPERIMENTAL	39
4.2.1 Materials	39
4.2.2 Synthesis of ZIF-8 Nanoparticles	40
4.2.3 Membrane Preparation	40
4.2.4 Phosphoric acid doping	41
4.3 CHARACTERIZATION	43
4.3.1 X-Ray Diffraction (XRD)	43
4.3.2 Fourier Transform Infrared Spectroscopy (FT-IR)	43
4.3.3 Scanning Electron Microscopy (SEM)	43
4.3.4 Proton Conductivity	43
4.4 RESULTS & DISCUSSIONS	44

4.4.1 X-Ray Diffraction (XRD).....	44
4.4.2 Fourier Transform Infrared Spectroscopy (FT-IR).....	45
4.4.3 Scanning Electron Microscopy (SEM)	46
4.4.4 Proton Conductivity	47
4.5 CONCLUSIONS	49
5. CONCLUSIONS	50

XRD
SEM

List of Figures

Figure 1.1 The total primary energy supply of world from 1971 to 2012.....	1
Figure 1.2 The total CO ₂ emission of world from 1990 to 2014.....	2
Figure 2.1.1 Electricity generation in a coal-fired thermal power plant.....	6
Figure 2.3.1 The structure of PEMFC and electrochemical reactions in it.....	8
Figure 2.3.2 PEMFC stack.....	10
Figure 2.3.1.1 Transport of gases, protons, and electrons in a PEM fuel cell electrode...	11
Figure 2.3.1 The structure of PEMFC and electrochemical reactions in it.....	14
Figure 2.4.1 Scheme of proton conduction mechanism.....	18
Figure 3.2.1.1 The chemical structures of the used chemicals.....	20
Figure 3.2.3.1 Scheme for preparation steps of the membranes.....	23
Figure 3.4.1.1 Comparison of XRD pattern of the membrane with ZIF-8 and without ZIF-8.....	24
Figure 3.4.1.2 XRD pattern of the different composite membranes and ZIF-8.....	26
Figure 3.4.2.1 FT-IR spectra of the different composite membranes.....	27
Figure 3.4.3.1 TGA thermograms of the different composite membrane and ZIF-8.....	28
Figure 3.4.4.1 SEM micrograph of ZIF-8 nanoparticles with higher magnification	29
Figure 3.4.4.2 Cross-sectional SEM micrograph of the membranes with different PAMPS loading.....	30
Figure 3.4.4.3 EDX element mapping for Zn and from the cross section of membrane with 55 PVA:10 PAMPS:5 ZIF-8 composition.....	32
Figure 3.4.5.1 Water uptake and IEC values of the membrane as a function of PAMPS content (%wt).....	34
Figure 4.1.1 poly [2,2'-(m-phenylene)-5,5'-bisbenzimidazole].....	41
Figure 4.2.3.1 Scheme for preparation steps of mixed matrix membranes.....	42
Figure 4.2.4.1 Photo of acid doped mixed matrix membrane.....	44
Figure 4.4.1.1 XRD pattern of ZIF-8 and mixed matrix membranes.....	46
Figure 4.4.2.1 FT-IR spectra of mixed matrix membranes.....	47
Figure 4.4.1.1 Arrhenius plot of MMM membranes.....	48

List of Tables

Table 2.2.1. The types of fuel cells.....	7
Table 3.4.51.1 Physicochemical properties of composite membranes	31
Table 4.4.1.1 Physicochemical properties of mixed matrix membranes	49



Chapter 1

Introduction

The energy demand of the communities and/or civilizations, which triggers their evolving, has increased since the dawn of civilization. By and large from the beginning of the industrial revolution up to now, the energy production systems/plants has undergone substantial change from low-power to power-intensive systems. While this evolution has positive impacts on our life such as transportation, health services, manufacture, it generates also several drawbacks and trouble for environment, access to energy and security and this has resulted in the rise of concern of energy. [1-4]

World* total primary energy supply from 1971 to 2012
by fuel (Mtoe)

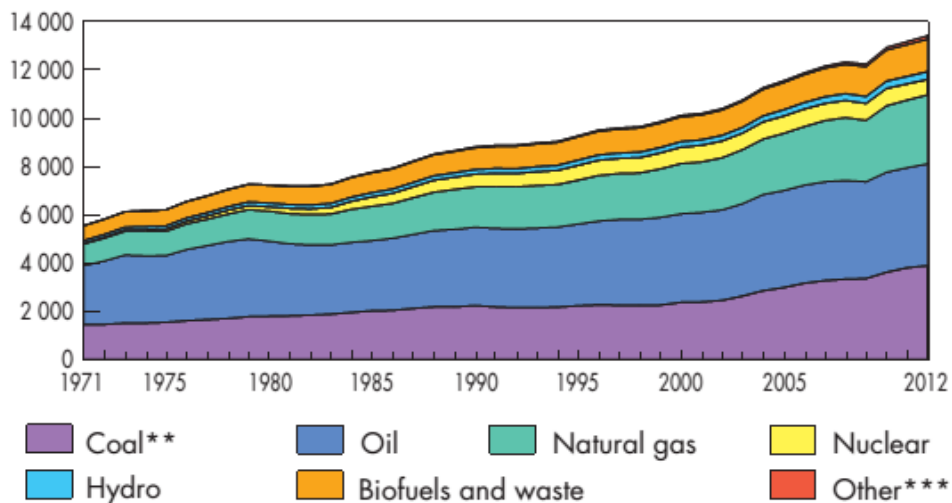


Figure 1.1 The total primary energy supply of world from 1971 to 2012 (*World includes international aviation and international marine bunkers.) [5]

Fig. 1.1 presents total change in total energy supply of world between 1971 and 2012. From this figure it can be seen that oil, coal and natural gas are the major energy sources, which roughly cover 80 % of the total energy supply, in given period. Thus three resources are called fossil fuels which originate in layers of prehistoric

carbonaceous materials that have been compressed over millions of years to form energy supplies. [5]

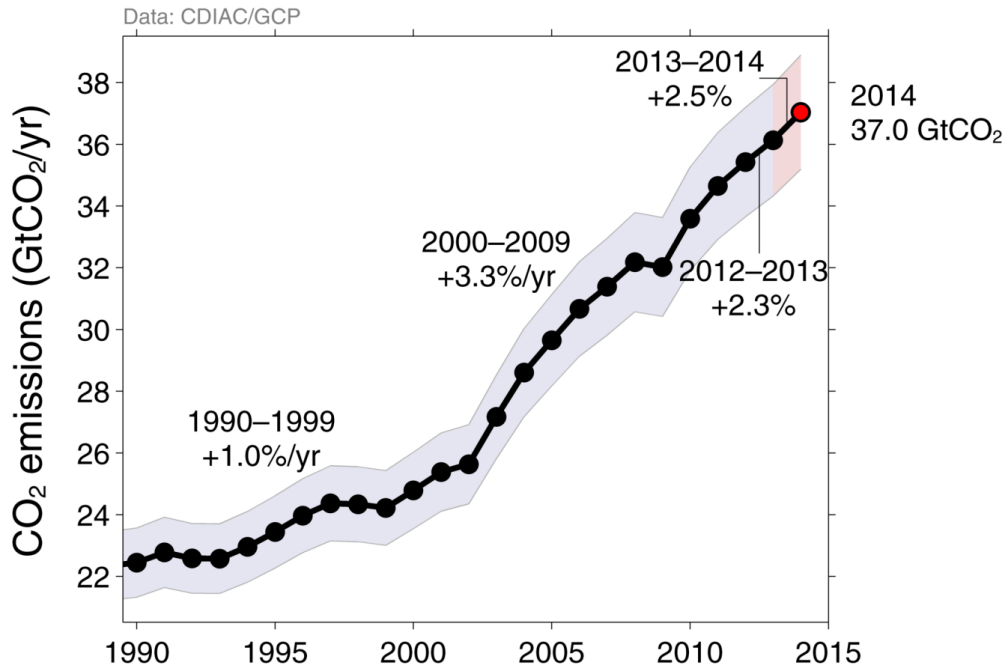


Figure 1.2 The total CO₂ emission of world from 1990 to 2014 (*World includes international aviation and international marine bunkers.)[6]

Different types of fossil fuels release different amounts of energy when they burn, as well as the almost total amount of emissions of pollution and greenhouse gases are emitted from the use of that energy.

The amount of the world CO₂ emissions, which is one of the greenhouse gases causing global warming, in terms of million tons for the same period is given in Fig. 1.2. Obviously as shown in Figure 2, emission values of CO₂ increased gradually from 1990 to the beginning of 2000s, but after this period emission rates dramatically increase due to the rising in the energy consumption of developing countries such as China and India. A report published on September 2014 by Global Carbon Project indicates that the world pumped 39.8 billion tons of CO₂ by burning oil, coal and natural gas. [6]Also, according to this report, China's per capita emissions had surpassed those of Europe for the first time, between 2013 and 2014.

Another report published by IEA claims that global energy demand increases by one-third from 2010 to 2035, with China and India accounting for 50% of the growth. [7] This means that unless alternative energy resources is used, the increasing trend in

emission of CO₂ will continue. According to this unpleasant scenario, with the increase of greenhouse gases in atmosphere the world will be uninhabitable for human beings in the next century.

In summary, our modern world meets its energy demand mainly from fossil fuels. To be dependent largely on fossil fuels brings out two big problems: energy security and environmental protection. Energy security comprises reliable access to supplies of all forms of energy; coal, oil, electricity, nuclear and renewable energy. The latter, environmental protection includes a special crack down on reducing greenhouse gas emissions –especially CO₂, which is the main cause of climate change. To struggle with these problems and to provide sustainability, alternative energy resources have to be discovered to diversify the fossil fuels and also to improve the efficiencies of current renewable technologies.

Proton exchange membrane fuel cells (PEMFCs) are one of the most innovative research areas in search of novel power sources, especially because of their no to low greenhouse gas emissions, high efficiency, diverse fuel options and low maintenance costs. Today, most common membranes are based on the perfluorosulfonic acid structure, and the well-known is Nafion, a trademark of Dupont. Nafion has a relatively high stability in mechanical terms and dimensions owing to its PTFE backbone, meanwhile, ionically bonded sulfonic acid functional groups enable protons to be transferred through the membrane. Nafion has such advantages, but it also has limitations and drawbacks such as high costs, methanol crossover and a rapid decrease in proton conductivity above 80 °C. Hence, commercialization of this PEMFC strongly depends on the investigation of novel proton exchange membranes with high proton conductivity, good thermal and chemical stability and cost-effective manufacturing. [1-4]

The main aim of this thesis is to prepare novel proton exchange membrane for PEMFC and high temperature PEMFC (HTPEMFC). In the manufacturing process of the membrane, composite membrane production methods were followed. All of the membranes were structurally characterized and further analysis was done for the usage as PEM. This thesis have five main sections as follows:

An outline of the research and the background and the motivations of the study are introduced in the First Chapter.

The main concepts of fuel cells and the main parts of the PEMFC are presented in Chapter Two. As well, proton conduction mechanisms through the PEM are discussed here.

Preparation and characterization of the composite membranes consisted of polyvinyl alcohol (PVA), Poly(2-acrylamido-2-methyl-1-propanesulfonic acid) (PAMPS) and Zeolitic Imidazolite Framework-8 (ZIF-8) are discussed in Chapter Three.

The preparation and characterization of the composite membranes consisted of Poly(benzimidazole) (PBI) and ZIF-8 are discussed in Chapter Four.

Final remarks on the results of this project and the recommendations for the future studies on PEM development are presented in Chapter Five under Conclusion.

Chapter 2

Introduction to Fuel Cells

Fuel cells are called the power source of the future. The interest in the fuel cells are increasing day by day since the fossil fuels have negative effects on the environment and cause problems for energy security because of limited resources and drillings in only certain parts of the earth, they do not have a future.

2.1 What is a fuel cell?

A conventional practice of electricity generation from fuels includes four steps as illustrated in Fig. 2.1.1: [1]

- i. Combustion of fuel converts chemical energy of fuel into heat
- ii. This heat is then used to boil water and generate steam
- iii. Steam is used to run a turbine in a process that converts thermal energy into mechanical energy.
- iv. Mechanical energy is used to run a generator that generates electricity.

At the third step of this process, conversion of thermal energy into mechanical energy occurs in a closed-cycle heat engine so the efficiency at this step is limited by Carnot cycle. Typical obtained efficiency from modern systems is about 41 %. Moreover, due to using mostly fossil fuels in the process, CO₂ and NO_x greenhouse gas emissions has increasingly adverse effects on the environment.

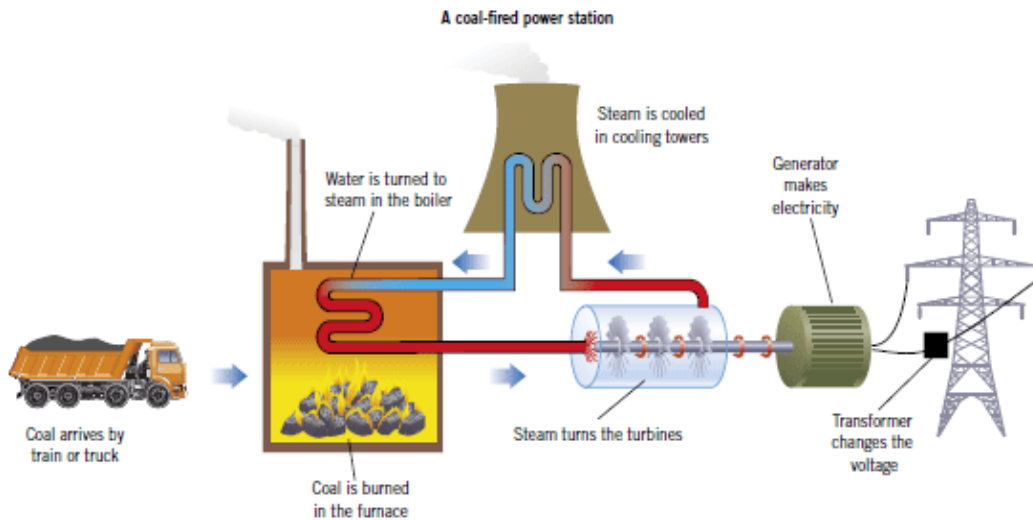


Figure 2.1.1 Electricity generation in a coal-fired thermal power plant [8]

Fuel cells show potential that they have the capability to substitute conventional energy conversion systems. A fuel cell, similar to a battery, converts chemical energy directly into electrical energy. A cell, which consists of three main parts called anode, electrolyte, and cathode, fed by hydrogen (or hydrogen-rich fuels) and oxygen (or air) produce electricity via electrochemical reactions. When oxygen and hydrogen are combined, activation energy reacts and forms water. This reaction that involves H_2 and O_2 is a combustion reaction so the reaction releases also some heat at the end of the process. In fuel cell, the direct reaction is hindered by the electrolyte and two half reactions occur at anode and cathode:

Anode: Fuel (H_2 or H rich fuels) is oxidized.

Cathode: Oxygen is reduced.

While the oxidized ions move through the electrolyte to the other electrode, the electrons are transported by way of in external wire. As a result of this partial reaction, the net electric current is obtained. In short, as the product of combustion reaction in fuel cell is a net electric current, the by-products of this reaction are heat and water. Therefore, from this aspect the fuel cells are environment-friendly energy generators in comparison with conventional plants. Moreover, conversion of chemical energy into electrical energy takes place at a single step in a fuel cell and because it contains no mobile parts, maintenance cost is considerably lower for these devices.

2.2 Types of fuel cells

Table 2.2.1 summarizes the different types of fuel cells. The primary different between each is type of electrolyte. Five main types of fuel cells are presented below:

Type of Fuel Cell	Electrolyte Membrane	Electrocatalysis	Operation Temp. (°C)	(Possible) Applications
Alkaline FC	KOH	Ni, Ag, Metal Oxides	120-250	Used in Apollo and Space Shuttle Program
Proton Exchange Membrane FC	Persulfonic acid membrane	Platinum/Carbon	60-80	Automotive applications, small-scale power generation
Phosphoric Acid FC	Phosphoric acid	Platinum	150-220	Stationary electricity generation (200 kW)
Molten Carbonate FC	Combination of alkali carbonates with a ceramic matrix	-	600-700	Demonstration stage
Solid Oxide FC	Non-porous Metal Oxide	-	800-1000	Portable power generation, auxiliary power in automobiles.

Table 2.2.1. The types of fuel cells

2.3 Proton exchange membrane fuel cell

The polymer electrolyte membrane fuel cell, also known as proton exchange membrane fuel cell, was first developed in General Electric Labs during the 1960s for NASA's Gemini program. [10] The fuel cells in this category use a polymer electrolyte membrane which is covered by highly dispersed catalyst particles on porous carbon. One-piece formed by/forming this structure is called membrane-electrode assembly (MEA).

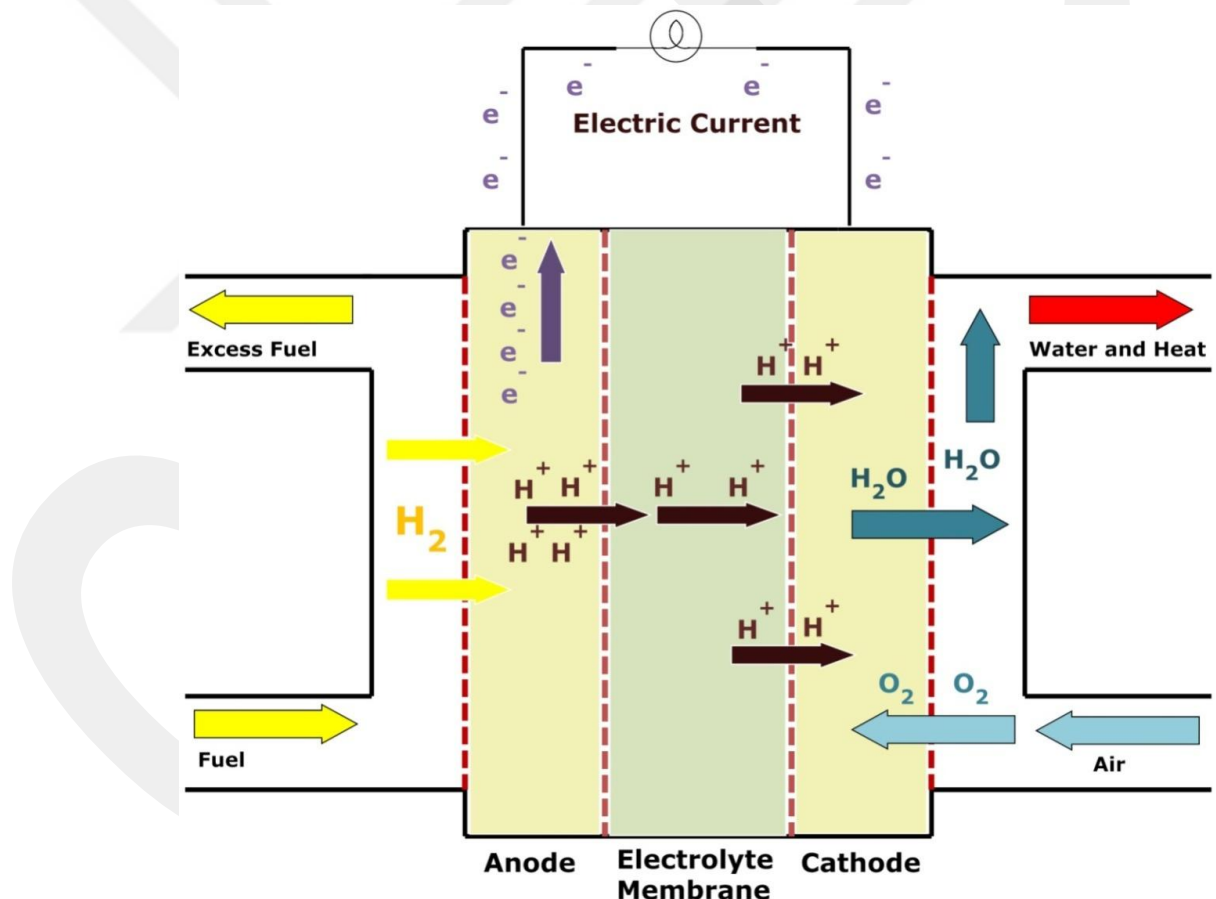
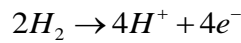
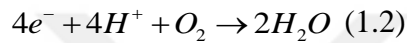


Figure 2.3.2 The structure of PEMFC and electrochemical reactions in it.

As shown in Figure 4, hydrogen is fed to the anode side of membrane (greater pressure than atmospheric pressure) where the catalyst causes the hydrogen atoms to release their electrons and to turn into H^+ ions (protons):



From the borders of the proton exchange membrane, only protons can pass through the assembly due to the semi-permeable structure of membrane. On the other hand, electrons are transported to cathode side by external circuit and as a result, a net electric current is obtained. At the cathode side, protons and electrons are combined with supplied oxygen (typically from air) to form water. As a result of this reaction some heat is released in energy form. The reaction at the cathode side is:



In addition, any excess fuel and oxygen are taken out the fuel cell's anode and cathode way outs, respectively. (Figure 4) The reaction in fuel cell carries on if only supply of fuel and oxygen (air) cease.

A fuel cell produces nearly 0.7 Volt electricity owing to the electrochemical reaction in it. Nevertheless, this value is far from enough to power turn out to account. So as to generate a useful voltage, a lot of single cells are connected as a fuel cell stack. This can be performed in a parallel and/or a series way to supply feed gas to the stacks. While all cells are fed in parallel from common hydrogen/air inlet in a parallel gas supply fuel cell stack, the gas from the outlet of the first cell is fed to the inlet of the second cell and so on until the last cell, which helps prevent non-uniform gas distribution. To avoid a large pressure drop, this arrangement can be used only for stacks with a small number of fuel cells. [1-4, 11]

Fig. 2.3.2 shows a typical fuel cell stack which is linked in series mode. In this structure each single cell is linked with an interconnect that is called bipolar plate. This plate has channels which provide to transport reactant gases (hydrogen and oxygen) to the electrodes. The electrically conductive bipolar plate is impermeable to gases and fluids; it can be performed as cooling plates as well.

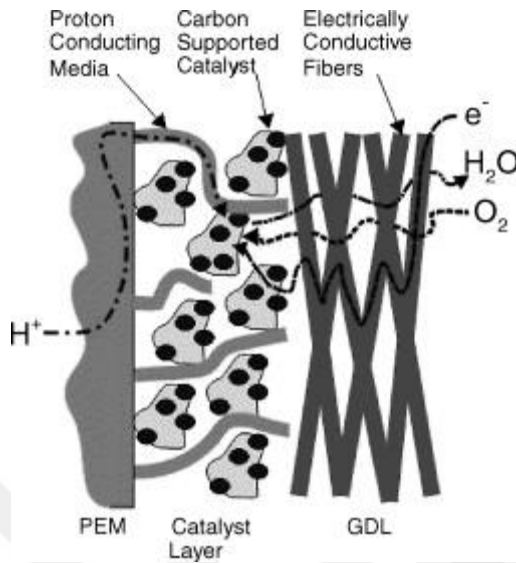


Figure 2.3.1.1 Transport of gases, protons, and electrons in a PEM fuel cell electrode [12]

The catalyst has a critical impact to reduce the activation barrier of the reaction. Platinum (Pt) or Pt alloy is common catalyst for both the anode and cathode reactions thanks to their well catalyst kinetics and highly unreactive behavior. In common usage, Pt or Pt alloy particles are dispersed on carbon support surface. Because of the transport phenomena on the CL, support material should have electrical conductivity and also show high thermal and chemical stability. But due to high costs, utilizing Pt or Pt alloys as catalyst in fuel cells increases the fabrication cost of fuel cell stacks. There are two major emerging researches to decrease Pt loading in fuel cells. The first one is to reduce particle dimensions and maximize effective surface area. The second is to investigate precious and non-precious new catalyst materials.

The structural and compositional properties of the CL in PEMFC are directly linked to the efficiency of the electrochemical reactions and the performance rates of the system. Hence, one of the major innovations in fuel cell technologies is developing CL in respect to these parameters. [1-4,11]

2.3.2 Gas Diffusion Layer

The union structure consists of a proton exchange membrane and both anode and cathode catalyst layers (CL) are called membrane electrode assembly (MEA). The MEA is sandwiched between two gas diffusion layers (GDL) which provide distribution of reactant gases to the operation area of the fuel cell. GDL is located between the bipolar plates and catalyst layers, so it enables for electrical conduction between the bipolar plate and electrode. In addition, GDL is a corridor for migration of reactant gases and taking away products, namely heat and water. A typical GDL has 100-300 μm thickness. The most common GDL material is the carbon fiber based porous structure, in addition to being used as hydrophobic materials (e.g. PTFE) in GDL they enhance water management through the MEA. [1-4,10-11]

2.3.3 Membrane

In a typical PEMFC, the main (core) part of the device is the polymer electrolyte membrane (PEM) which provides conducting of protons (H^+) from cathode to anode. An ideal PEM possesses high proton conductivity however it shows lower electronic conductivity than electrically isolate anode and cathode components, so electrons are transported by an external circuit to generate electricity. The membrane should be impermeable to gases (oxygen and/or fuel) for both sides of the membrane under the operation conditions. In addition, it should show good mechanical properties in both dry and hydrated states and also have well oxidative and hydrolytic stability. Lastly, the membrane material should have capability for fabrication into membrane electrode assemblies (MEA), and the materials which are parts of the membrane should be cost effective for commercialization of product.

Today, the most common membranes are based on the perfluorosulfonic acid structure, and the well-known is Nafion®, a trademark of Dupont™.

Nafion®, has a relatively high stability in mechanical terms and dimensions owing to its PTFE backbone, meanwhile, ionically bonded sulfonic acid functional groups enable protons to be transferred through the membrane. Furthermore, several perfluorinated polymer materials such as Flemion™ (Asahi Glass Company), Gore-Select™ (W.L. Gore and Associates, Inc.), Neosepta-F™ (Tokuyama), Asiplex™ (Asahi Chemical Industry) are also modified for use in PEM fuel cell applications.

Nafion® has some advantages; nevertheless it also has limitations and drawbacks. One of the disadvantages of the Nafion® is its high-price because of its complex production process. On the other hand, proton conductivity through the Nafion® very contingents on the water uptake values of the membrane. By virtue of the fact that high water uptake ratio brings about high proton conductivity, the membrane should be wetted sufficiently to obtain high proton conductivity. However, due to the rapid dehydration above 80 °C, the proton conductivity of the membrane decreases, therefore the operation conditions of the Nafion® is limited up to 80 °C. [13]

The shortcomings originating from using of Nafion® in PEMFC were surpassed by utilizing heterocyclic aromatic polymers as PEM. Phosphoric acid doped- polybenzimidazole (PBI) membrane is the auspicious material owing to thermally stable at high temperatures, good proton conduction up to 200 °C and lower methanol crossover. Polybenzimidazole refer to a large family of heterocyclic polymers consist of benzimidazole units. Since PBI has poor intrinsic proton conductivity, it needs to be doped with some acids to enhance its proton conductivity for fuel cell applications. Therefore, the proton conductivity of the PBI membranes strongly depends on the acid content in the membrane. Phosphoric acid is mostly used as doping agent because phosphoric acid doped membrane has higher proton conductivity compared with other acid doped membranes. However, for needed cold start operation, poor proton conductivity at low temperatures. And also non-bonded acid inside the membrane can cause the acid leakage through the membrane and this can damage the electrodes and gas diffusion layers (GDL).[14-15]

2.4 Proton Transfer Mechanism

One of the most important cases in the fuel cell is proton conduction through the membrane. This phenomena is linked with both acid and water content of the membrane, it is also influenced by the strength of the acid, the morphology and chemical structure of the membrane, and the temperature of the medium.

Proton conduction through the membrane in the PEMFC is explained by two mechanisms: Grotthuss-type and vehicle-type mechanisms.

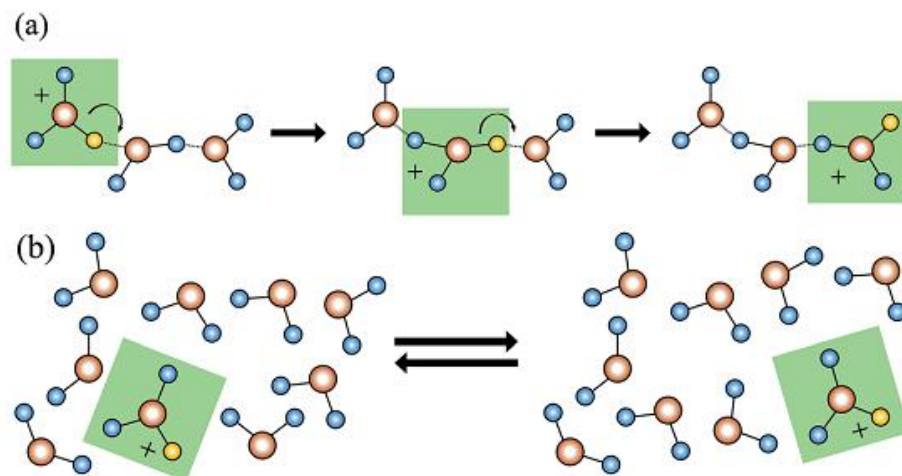


Figure 2.4.1 Scheme of proton conduction mechanism: (a) Grotthuss-type mechanism ;(b)Vehicle-type mechanism

2.4.1 Grotthuss-Type Mechanism

In the case of proton conduction mechanism via Grotthuss mechanism, proton migration from one site to the another is controlled by the formation and breaking of hydrogen bonds between a hydronium ion. As shown in Fig. 2.4.1 (a), protons hop from one hydrolyzed ionic site to another; this phenomena is also called proton hopping. During the proton transferring from one site to

another site, two important states occur: rearrangement and reorientation, which are determined by two potential wells, related to the proton donor and proton acceptor. The energy difference between the potential wells is in the order of a few kJ mol^{-1} . In a system with strong hydrogen bond is resulted in low activation energy with high proton conductivity.

2.4.2 Vehicle-Type Mechanism

In the vehicle-type mechanism, a proton combines with solvent molecules in the medium, produces a complex and then diffuses. For instance, a proton combined with water molecule in the medium can migrate by hydronium ion (H_3O^+). This is illustrated in Figure 2.4.1 (b). In this process, solvent molecules act as vehicle which of carried of protons. Diffusion rate is determined by a gradient in proton concentration. And observed conductivity is the rate of vehicle diffusion. In this type proton transfer, some drawbacks arise due to the inherent structure of the process. For example, the hydrogen bonding between the water molecules causes the decreasing of diffusion rate of hydronium ions. In comparison with hopping mechanism, diffusion process is far slower and is marked by a higher activation energy and lower proton mobility.

Chapter 3

Proton Conducting Nafion-Like Ternary PVA/PAMPS/ZIF-8 Composite Membranes

3.1 Literature Survey

Physically blended membranes that consist of hydrocarbon matrix are significantly draw attention because of being cost-effective and showing high water selectivity as well as they are highly impermeable to methanol. PVA is widely used as a matrix component in blended membranes because of its well forming film ability, hydrophilic structure, chemical and mechanical stability. [17-25] However, PVA can be dissolved in water even at room temperature, yet thankfully –OH functional groups in its structure, PVA can be cross-linked chemically by aldehydes resulting in remarkable improvement in connection with thermal and mechanical stabilities.[32-35] Another drawback of the PVA that restrains the using singly in fuel cell membrane is having poor proton conductivity. [24,40]

PAMPS, which is derived from AMPS (2-acrylamido-2-methylpropanesulfonic acid), is an acidic polymer that shows a higher proton conductivity than partially hydrated Nafion. [56] As a result of chemical structure, PAMPS is able to exhibit much endurance of water in comparison to Nafion and polystyrene sulfonic acid (PSSA). Therefore it can be suitable membrane materials for fuel cell operation at high temperatures. [56] But for all that, since PAMPS homopolymer is suffered from water, it could not be use as pristine form in a membrane.

MOFs -metal organic frameworks - ,which are a new class of ordered porous materials, are consist of inorganic metal clusters and organic linkers. [47] Since they could be designed for the desire function by tailoring, MOFs attract much attention from diverse research disciplines. In addition to gas adsorption and separation, catalysis, sensing and gas storage properties of MOFs, there have been greater effort on proton conducting properties of such materials. To obtain proton conductive MOF, there are three major options in the literature: (I) to construct proton pathways by the rational selection of metal clusters and organic linkers, (II) to introduce acidic and hydrophilic units into MOFs pores, (III) to include stronger acids -such as sulfuric acid and phosphoric acid- into porous structure. [46-48]

The goal of this study is to synthesize new composite proton exchange membranes with high proton conductivity, good chemical and mechanical properties. To do this, PEMs were synthesized by physically blended and cast. PVA is the main matrix material in the composite membrane due to its well film-forming ability and mechanical properties. To enhance its swelling properties, cross-linking via glutaraldehyde, in which chemical cross-linking reactions between hydroxyl groups (-OH) of PVA and the aldehyde groups (-CHO) of GA, is feasible method. PAMPS is not only primary proton donor in the membrane but also it is catalyst for the acetalization reaction as an alternative of conventional HCl. Zeolitic Imidazolat Frameworks (ZIFs) are a sub-class of MOFs which have akin to pore topologies with zeolites and show superior chemical and thermal stability. ZIF-8 consists of Zn (II) metal cation linking with 2-methylimidazolate (Hmim) anion in the tetrahedral framework that forms the sodalite (SOD) zeolite structure with large cavities (11.6 Å) and small pore size (3.4 Å). As a result of Hmim linkers, ZIF-8 is vastly hydrophobic that provides a high water stability for the framework in make contact with the water. In consequence of hydrophobic nature and better compatibility with polymer matrix, ZIF-8 is anticipated to improve water management of the membrane, and also it can assist for the proton conduction.

3.2 Experimental

3.2.1 Materials

2-Methylimidazole (Hmim with 97% purity), Zinc Nitrate Hexahydrate ($\text{Zn}(\text{NO}_3)_2 \cdot 6\text{H}_2\text{O}$, 99% purity – metal based) were both purchased from Alfa Aesar. PAMPS ($M_w = 2\,000\,000$, 15 wt % in aqueous), PVA ($M_w = 89\,000 - 98\,000$, more than 99% hydrolyzed), Gluturaldehyde Solution (GA, 25 wt % aqueous) were all purchased from Sigma-Aldrich. Methanol with 99.9 % purity was purchased from Merck. (Fig. 3.2.1.1)

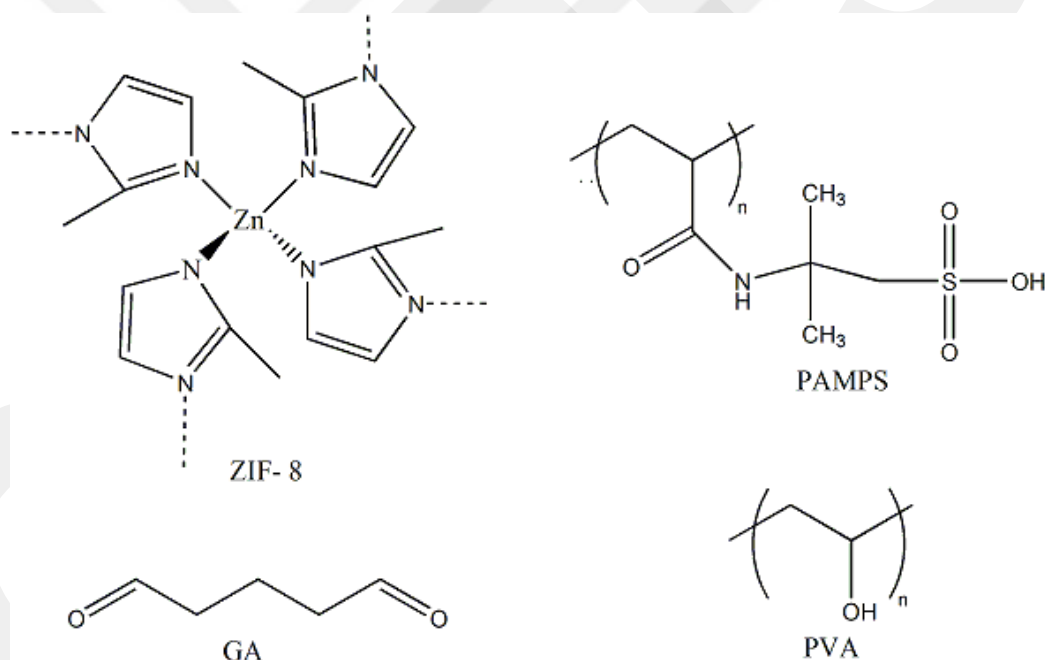


Figure 3.2.1.1 The chemical structures of the used chemicals

3.2.2 Synthesis of ZIF-8 nanoparticles

In the synthesis of the ZIF-8 nanoparticles, the same procedure was followed which is described by Cravillion et al. [45] Shortly, 1.0510 g (3.53 mmol) $\text{Zn}(\text{NO}_3)_2 \cdot 6\text{H}_2\text{O}$ was dissolved in 50 ml methanol and 2.3353 g (28.3 mmol) Hmim was dissolved in 50 ml methanol. Then first solution was poured into second solution. And the final solution was vigorously stirred room temperature for 1 h. At the end of the stirring process, the milky solution was

centrifugated at 7500 rpm two times and nanoparticles were washed by methanol. The yield of ZIF-8 was ~30 % based on Zn. Afterward; some were heated in the vacuum oven at 80 °C during 24 h for further characterization. The rest of nanoparticles were kept in methanol during all next steps. The yield of ZIF-8 was ~30 % based on Zn.

3.2.3 Membrane Preparation

The PVA/PAMPS/ZIF-8 mixed matrix membrane was prepared by solution casting method. 1.25 g powder PVA was dissolved in 40 ml distilled water and solution was stirred at 70 °C for 3 h. ZIF-8 in methanol (0.096 g ZIF-8) was poured into PVA solution after solution was cooled down at room temperature. The suspension was then stirred for 12 h strongly. Afterward, certain amount of PAMPS solutions were added to prepared solution and this solution was stirred vigorously for 12 h at room temperature. The cross-linking was carried out in situ by adding 0.1 M GA (25 % wt in water), no acidic reagent was added as catalyst owing to PAMPS. [36] As the final step, the blend was cast onto a glass petri dish. The casting films were put in hood under ventilation during the overnight. Finally, films were put into vacuum oven at 70 °C for 4 h to evaporate the residual solvent. The final concentration of the PAMPS to all film was varied at 0, 10, 20, 30, 40 wt %. (Fig.3.2.3.1)

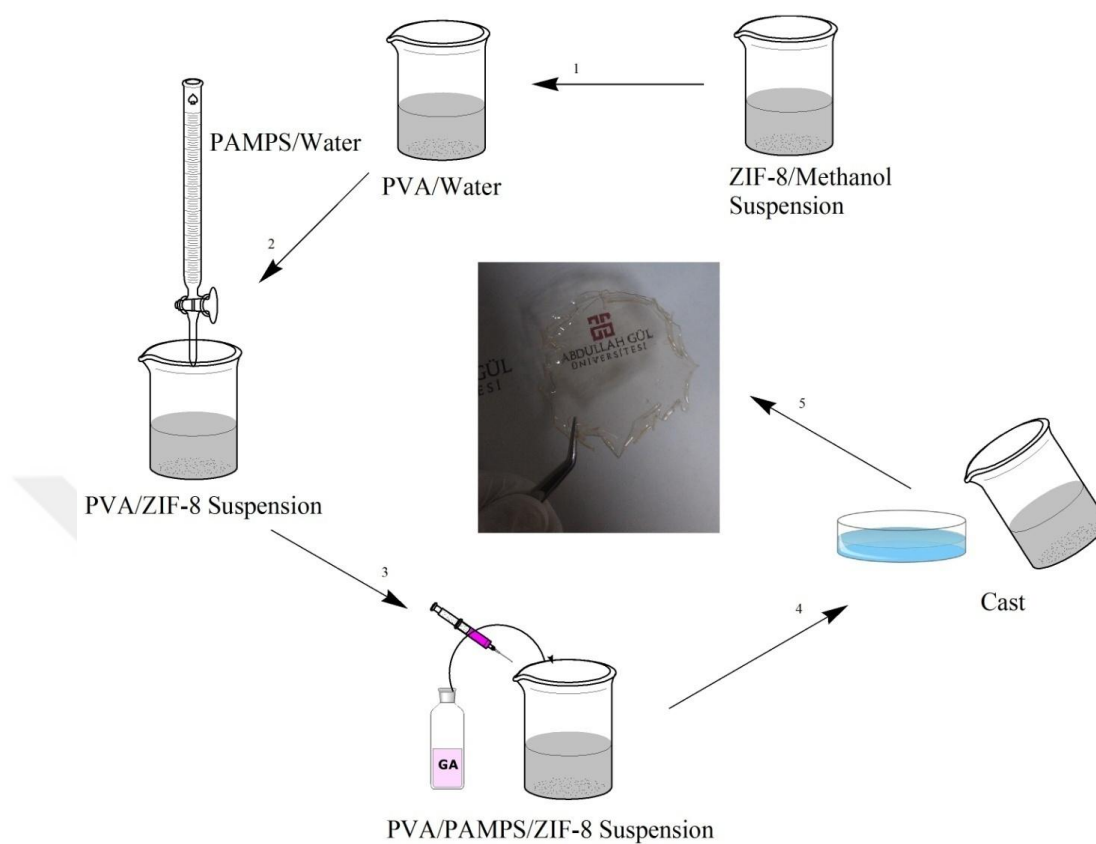


Figure 3.2.3.1 Scheme for preparation steps of the membranes

3.3 Characterization

3.3.1 X-Ray Diffraction (XRD)

X-ray diffraction pattern of the prepared membranes were acquired by using Bruker AXS D8 Advance. The diffraction angle (2θ) range from 5° to 40° was scanned at a scan rate $0.01^{\circ} \text{ min}^{-1}$ with 1.54 nm wavelength radiation which is generated by $\text{CuK}\alpha$.

3.3.2 Fourier Transform Infrared Spectroscopy (FT-IR)

The prepared membrane was examined by using Attenuated Total Reflectance Fourier Transform Spectroscopy (ATR-FTIR) on Thermo Nicolet 6700. Spectrum was obtained with 4 cm^{-1} resolution between $400 - 4000\text{ cm}^{-1}$.

3.3.3 Thermo-gravimetric Analysis (TGA)

Thermal degradation of the membranes and ZIF-8 nanoparticles was examined by Shimadzu DTG 60. All the thermal measurements were carried out under the nitrogen atmosphere and the $10\text{ }^{\circ}\text{C min}^{-1}$.

3.3.4 Scanning Electron Microscopy (SEM)

The morphologies of the prepared membranes were examined by Zeiss EVO LS 10. To affirm the existence and homogenous distributions of the ZIF-8 nanoparticles in the composite membrane, elemental mapping was carried out via energy-dispersive X-ray spectroscopy.

3.3.5 Proton Conductivity

Proton conductivity measurements of the prepared membranes were performed via using a Novocontrol dielectric-impedance analyzer. The films were sandwiched between platinum blocking electrodes and the conductivity was measured in the frequency range from 1 Hz to 3 MHz as a function of temperature, which was varied from $20\text{ }^{\circ}\text{C}$ to $80\text{ }^{\circ}\text{C}$ in $20\text{ }^{\circ}\text{C}$ intervals.

3.3.6 Water Uptake (WU)

The water uptake studies of the prepared membranes were performed in the following procedure: Square pieces membranes samples which were certain dimension were dried at $65\text{ }^{\circ}\text{C}$ to evaporate residual solvent and weighed. Then dry membranes were soaked in deionized water for 24 h, surface water properly wiped by filter paper and weighed. And water uptake of the membranes found out using equation:

$$\text{Water uptake} = \frac{W_{\text{wet}} - W_{\text{dry}}}{W_{\text{dry}}} \quad (3.3.6.1)$$

where W_{wet} and W_{dry} are the wet and dry mass of the membranes.

3.3.7 Ion Exchange Capacity (IEC)

The ion exchange capacity (IEC) values of the prepared membranes were determined by titration which is reported (ref). Firstly the samples pieces were cut off prepared membranes were dried at 65⁰C under vacuum. Then membranes were immersed in a 25 mL with 2 M NaCl aqueous solution to replace the H⁺ by Na ions. Afterward; the solution was titrated with 0.1 M NaOH solution as using phenolphthalein indicator. The IEC is expressed in terms of milliequivalents of sulfonic groups per gram of dried sample.

3.4 Results and Discussions

3.4.1 X-Ray Diffraction (XRD)

XRD patterns of synthesized ZIF-8 and membranes with different PAMPS loadings are shown in Fig. 3.4.1.2. The peaks on the pattern of the ZIF-8 nanoparticles go with XRD pattern in the literature, correspondingly. Cross-linked blended membranes shows two observable peak around at 2 θ of 20⁰ and 35⁰. The sharp peak about 20⁰ corresponds to (101) plane of the semi-crystallized PVA. [40,45,46] As observed Fig. 3.4.1.2, there are no agglomerations in the blended membranes which contain ZIF-8, since the ratio of ZIF-8 in mass is very low and ZIF-8 nanoparticles well distributed in the membrane because of their partially organic nature. On the other hand, Fig. 3.4.1.1 prove the existence of the ZIF-8 nanoparticles in the membrane. In comparison with the pattern of 60PVA: 40PAMPS membrane, there are some weak peak, which appears in 2 θ of 14.40⁰, 17.96⁰, 19.12⁰ and 27.50⁰, on the pattern of 55PVA: 40PAMPS: 5ZIF-8 membrane. This is illustrated in Fig. 3.4.1.1. And also, the membrane consisting of ZIF-8 has relatively higher

intensity peak about at 2θ of 20° than the membrane consisting of only PVA and PAMPS. The most likely explanation of these results is that ZIF-8 nanoparticles in the membrane perform as nucleation sites and this is resulting in improving crystallinity of the membrane. [40] PAMPS has no crystal phase and it is almost in amorphous phase. [56]

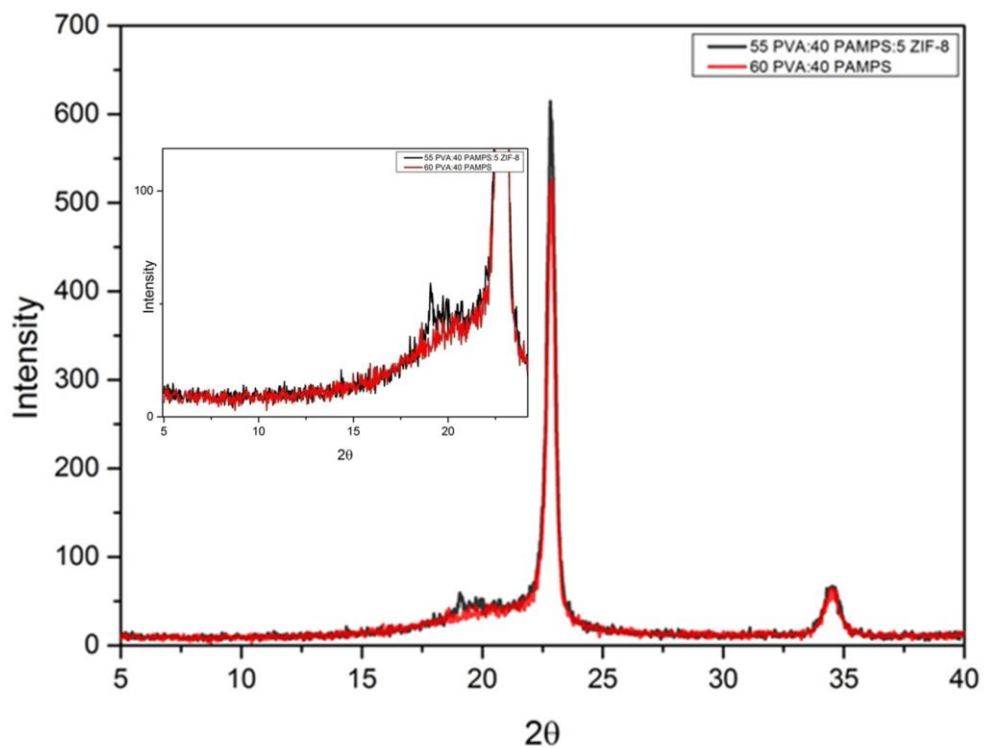


Figure 3.4.1.1 Comparison of XRD pattern of the membrane with ZIF-8 and without ZIF-8

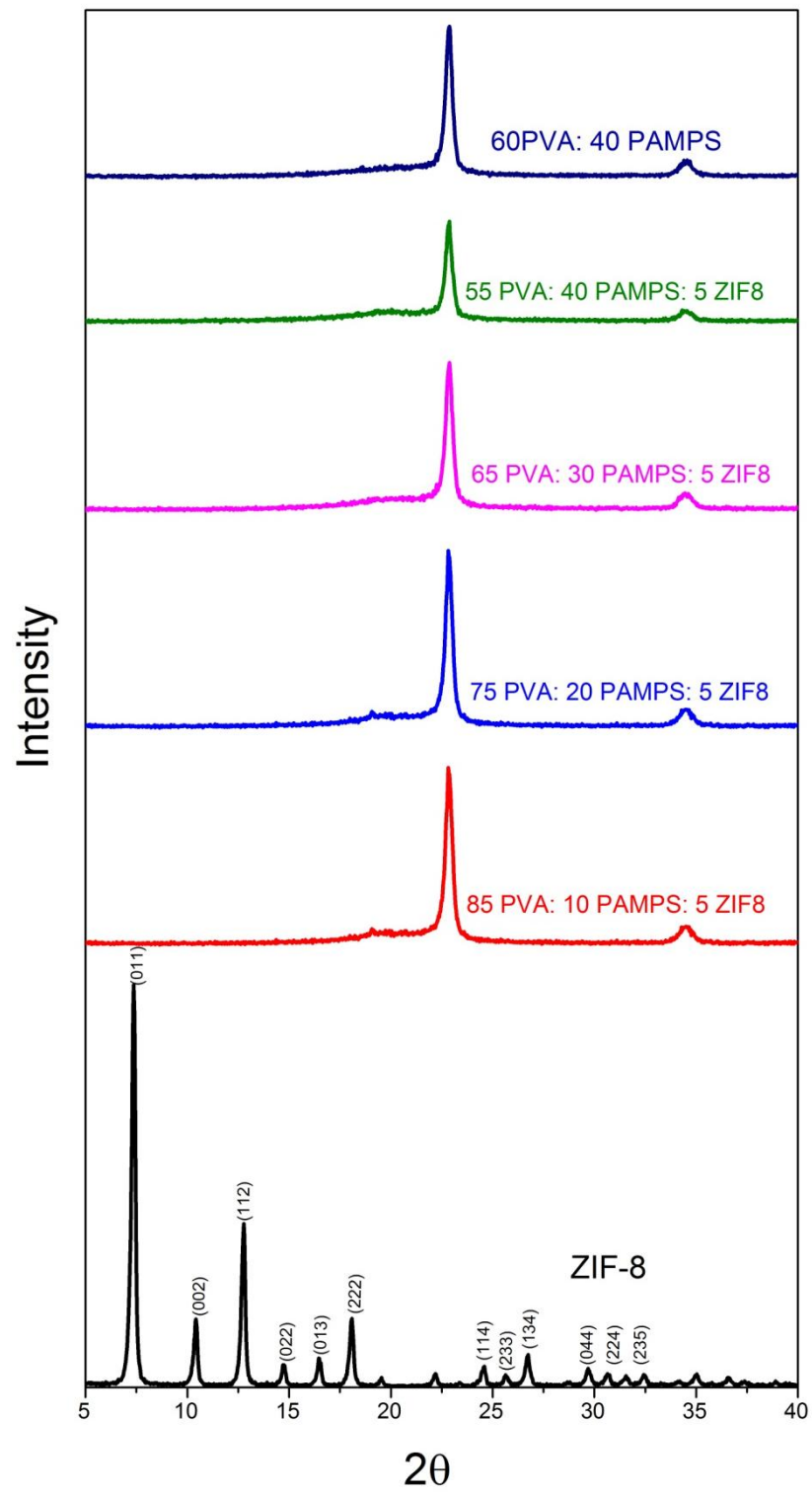


Figure 3.4.1.2 XRD pattern of the different composite membranes and ZIF-8

3.4.2 Fourier Transform Infrared Spectroscopy (FT-IR)

ATR/FT-IR was used in order to determine intermolecular and/or interchain hydrogen bonding between host polymers and ZIF-8 nanoparticles, and to identify the existence of crosslinking reactions between PVA and GA. Transmittance FT-IR spectra of the PVA/PAMPS/ZIF-8 ternary membranes and PVA/PAMPS binary membrane are shown in Fig 3.4.2.1. The absorption peaks occurred in all spectra around at 3306 cm^{-1} and 2930 cm^{-1} are associated with (O-H) stretching and asymmetrical stretching of methylene (C-H) group in PVA chains, respectively. [18,25] The sharp peaks at about 1650 cm^{-1} and 1545 cm^{-1} are assigned to vibration of (C=O) and (N-H) group in PAMPS. While the intensity of signal come from (C=O) group increases with increasing of PAMPS content in the all membrane,[32-39] the vibration peak of (N-H) groups dwindles with the increasing of PAMPS content in the ZIF-8 contained ternary membranes. The possible justification to this result is occurring of intermolecular hydrogen bonding between non-defect-free ZIF-8 nanoparticles and (N-H) groups in the PAMPS chains. Additionally, as can be seen from Fig. 3.4.2.1 the sharp peaks come about around at 1021 and 1112 cm^{-1} are corresponded to (S-O) stretching of sulfonic acid groups in PAMPS. As well, the weak signal at around 835 cm^{-1} are attributed to the bending of (O-H) because of the free (-CHO) group that are sourced from excess GA.[36]

However, the characteristic peaks of the ZIF-8 could not be seen in this spectra. The reasons are that too few ZIF-8 contents in the membranes and the overlapping of characteristic peaks of ZIF-8 with the polymer hosts. For instance, while the taking placed at $3125 - 2929\text{ cm}^{-1}$ aromatic aliphatic (C-H) stretch of imidazole [40, 45] belonged to ZIF-8 is overlapped by the broad (O-H) stretch of PVA, the (N=C) stretching of ZIF-8 coincides with vibrations of amide groups in PAMPS. On the other hand, the formation of hydrogen bond between hydroxyl groups of PVA and sulfonic acid groups in PAMPS could not be determined independently due to the overlapping hydrogen bonding between $\text{SO}_3\text{H} - \text{OH}$ and $\text{OH} - \text{OH}$. [20]

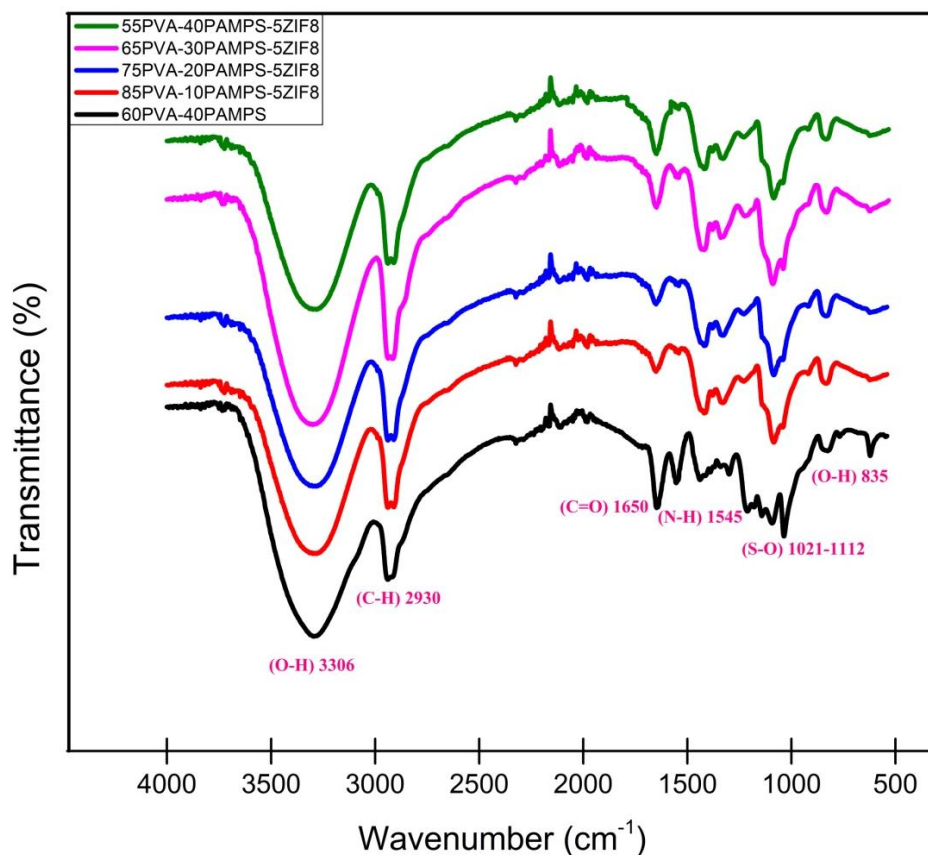


Figure 3.4.2.1 FT-IR spectra of the different composite membranes

3.4.3 Thermo-Gravimetric Analysis (TGA)

Fig. 3.4.3.1 shows thermal degradation thermograms of the membranes containing PVA-PAMPS-ZIF-8 membranes by changing the PAMPS and PVA content and pure ZIF-8. The membrane samples were dried in a vacuum at 80 °C and hold on vacuum until measurement. From this figure, three major stages of the thermal decomposition can be considered for the membranes. The first stage of the decomposition, which occurs between 150 and 230 °C, is the degradation of the sulfonic acid groups (-SO₃H) in PAMPS. [18,20,29,35] The second decomposition stage begins at around 230 °C and ceases at about 350 °C, which is attributed to cleavage of the side-chain of PVA. [23,25] And the final

major decomposition step comes about between 330 and 540 °C, which is ascribed to cleavage of the backbone of the PVA. As presented in Fig. 3.4.3.1 a long plateau occurred up to 500 °C is sign of the high thermal stability of the ZIF-8 nanoparticles.[40,45] A gradual weight loss about 8 % wt is linking with the subtraction of residual solvents or reactant molecules trapped in the nanocrystals during synthesis.

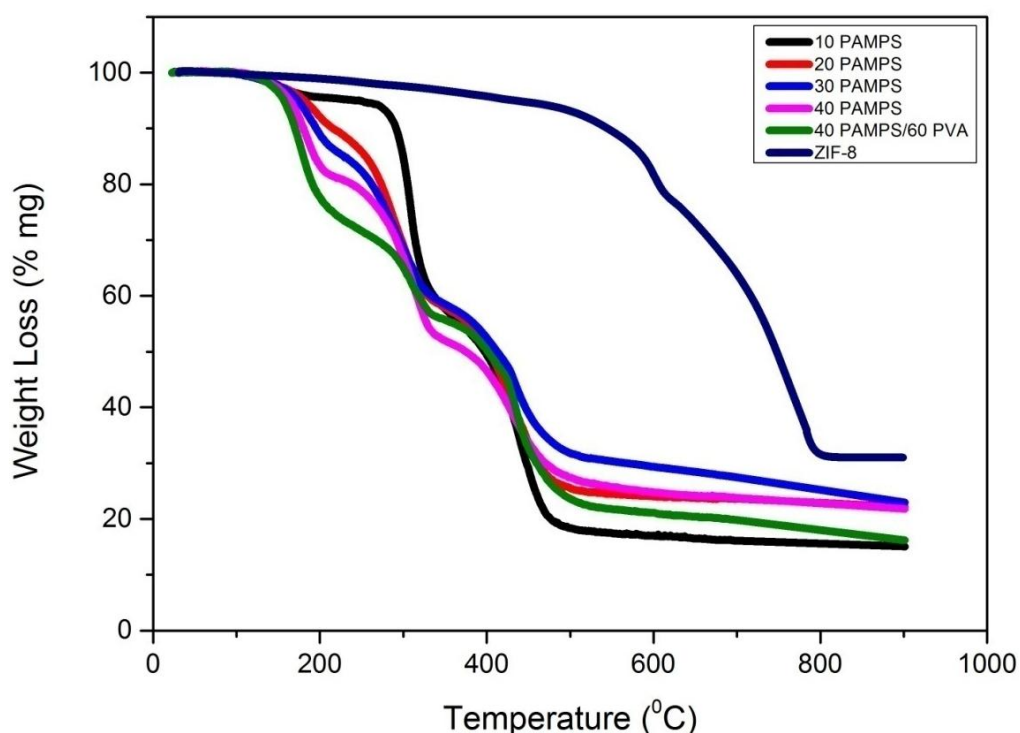


Figure 3.4.3.1 TGA thermograms of the different composite membrane and ZIF-8

In this work and in related references it was observed that the pure PVA polymer remains stable up to 300 °C but with the addition of PAMPS, blends membranes exhibited a lower thermal stability. For higher PAMPS content in the membranes bring about an early start decomposition, nevertheless loss in weight gets gradual. The differences in PAMPS content and existing of ZIF-8 nanoparticles in the membranes result in significant differences in total weight drops of the blends membranes. For instance, remained mass of the composition, PVA:PAMPS:ZIF-8 = 85:10:5 in weight, was much lower than that of the

PVA:PAMPS:ZIF-8=55:40:5 in weight. Moreover, the total weight drops in all of composition of contained ZIF-8 -except consisting of 10 wt % PAMPS membrane- are considerably lower than PVA:PAMPS = 60:40 in weight. An important implications of these findings that there is an interaction between PAMPS and ZIF-8.

3.4.4 Scanning Electron Microscopy

Fig. 3.4.4.1 presents the SEM images of the synthesized ZIF-8 nanoparticles. As can be seen from Fig. X, the size of the nanoparticles varies from 40 nm to 60 nm.

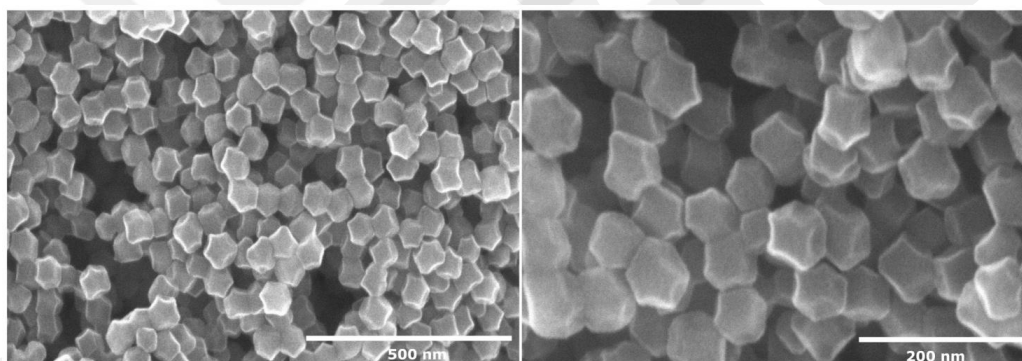


Figure 3.4.4.1 SEM micrograph of ZIF-8 nanoparticles with higher magnification (100k ×)

Cross sectional SEM micrographs of the blended membrane for different PAMPS loadings are given in Fig. 3.4.4.2. Apparently, existence of the ZIF-8 nanoparticles in the membrane did not cause any considerable changes on the morphology of the membranes, due to the low content of ZIF-8 through membranes. From this we conclude that ZIF-8 nanoparticles homogeneously distributed through the membrane. The cross-sectional micrographs prove that there are any voids or agglomeration at the inter-phase regions.

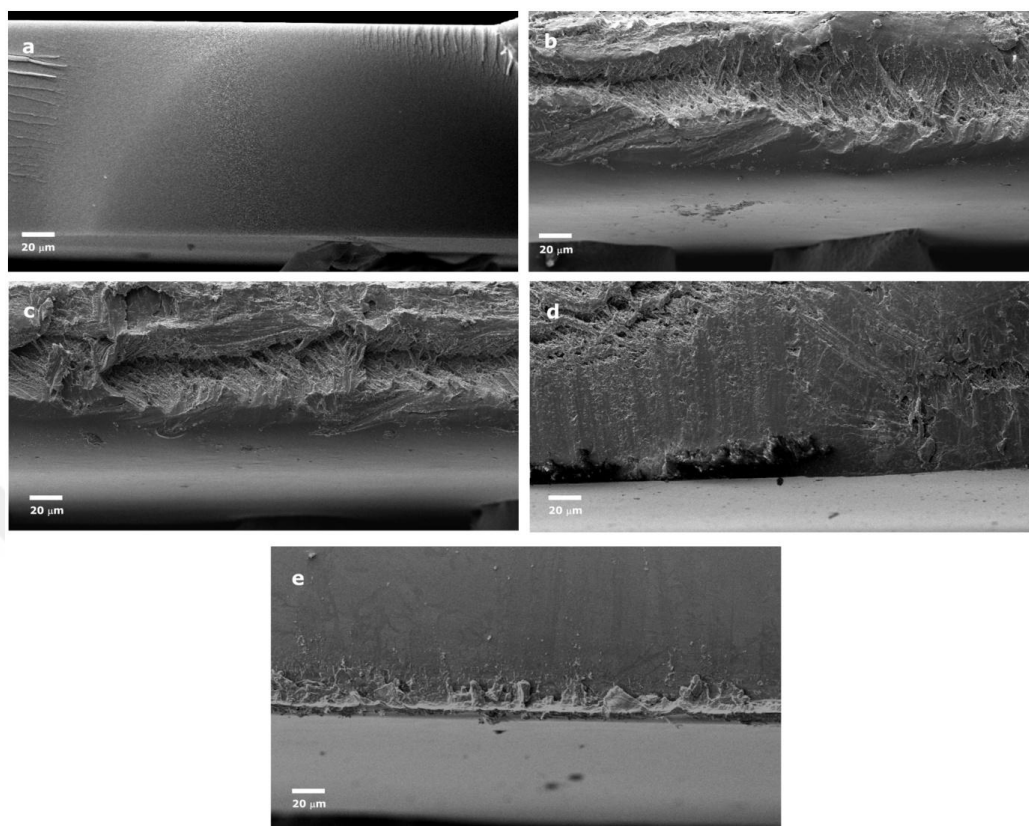


Figure 3.4.4.2 Cross-sectional SEM micrograph of the membranes with different PAMPS loading (magnification of 2500 ×): (a) 60 PVA:40 PAMPS, (b) 85 PVA:10 PAMPS:5 ZIF-8, (c) 75 PVA:20 PAMPS:5 ZIF-8, (d) 65 PVA:10 PAMPS:5 ZIF-8, (e) 55 PVA:10 PAMPS:5 ZIF-8

Fig. 3.4.4.3 reconfirms the homogenous distribution of ZIF-8 nanoparticles through the membrane by mapping Zn and S elements with using of the energy dispersive x-ray spectroscopy. As can be seen from EDX mapping micrographs Zn element has an uniform distribution in the composite membrane. The results obtained from EDX mapping prove that ZIF-8 nanoparticles uniformly distributed in the membrane because zinc elements only exist in ZIF-8. Additionally, with this approach these results also indicate that the distribution of the PAMPS is homogenous in the membrane.

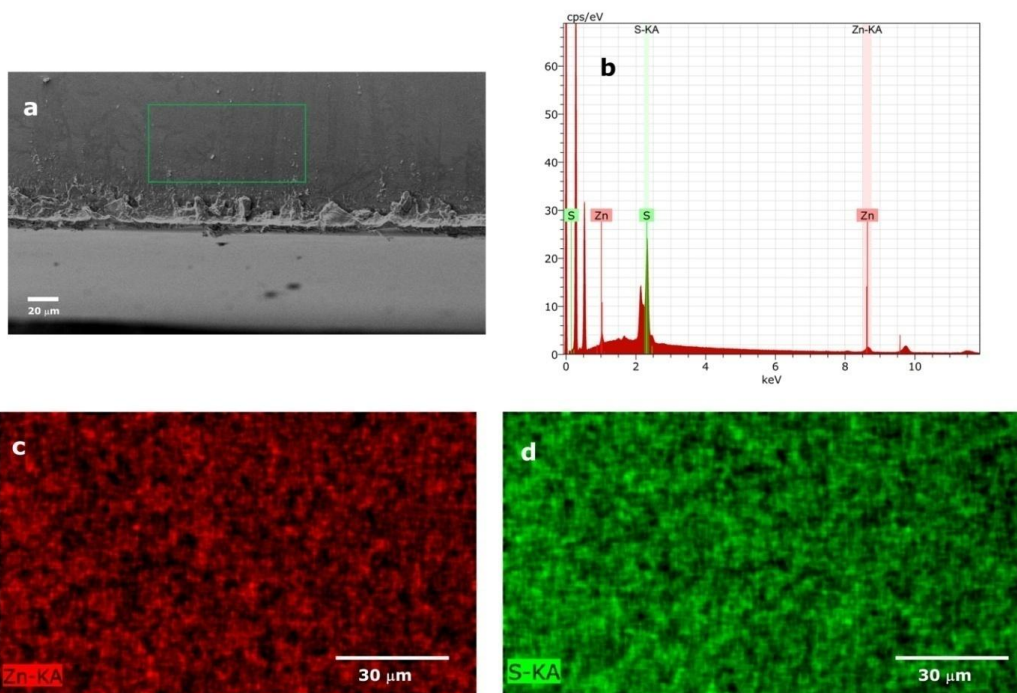


Figure 3.4.4.3 EDX element mapping for Zn and from the cross section of membrane with 55 PVA:10 PAMPS:5 ZIF-8 composition. (magnification of 2500 ×)

3.4.5 Water Uptake (WU) and Ion Exchange Capacity (IEC)

The water uptake (WU), in other words swelling behavior, has a significant function for both migration of the protons along the membrane and the dimensional stability of the membrane under the operation conditions. [18,24,28]The high water uptake values for the membranes serve high proton conducting. Yet, the excessive water uptake values in the membranes can cause some weakness on dimensions of the membranes and their thermal properties. The water uptake values of the membranes are shown in Table 3.4.5.1. The hydrophilic parts in the membranes majorly determine water uptake values of the membrane. Obviously PVA is instable polymer in water due to hydrophilic (-OH) functional groups, but the polymer gain flexibility and mechanical strength via chemical cross-linking. On the other hand, because of the imidazole linkers, ZIF-8 shows natural hydrophobic properties. [74-76]Hence, the water uptake values of the membrane is majorly changed by the PAMPS content in the

membrane. It is well known that sulfonic acid groups (SO_3H) are highly hydrophilic. [34-36] Therefore, as can be seen in Table 3.4.5.1, the WU values are increasing with the increasing of PAMPS contents in the membranes. The measured water uptake values increase from 2.13 to 3.28. However, in comparison with 60 PVA: 40 PAMPS, the membrane with 55 PVA: 40 PAMPS: 5 ZIF-8 has slightly higher water uptake. The reason is that adsorbed water in ZIF-8 pores increase the water uptake values of the membrane despite the hydrophobic nature of the ZIF-8.

PVA:PAMPS:ZIF-8 Ratio (wt %)	IEC (meq/g)	Water Uptake	Proton Conductivity (S/cm)	Activation Energy (kJ/mol)
85:10:5	0,34	2,13	0,001	10,81
75:20:5	0,54	2,43	0,005	11,40
65:30:5	1,12	3,01	0,084	12,46
55:40:5	1,52	3,28	0,134	15,23
60:40	1,54	3,05	0,104	12,26

Table 3.4.52.1 Physicochemical properties of composite membranes

The number of exchangeable ion groups in the membrane is determined by ion exchange capacity (IEC) of the membrane. Generally, IEC is given in terms of the moles of fixed SO_3^{-1} sites per gram of polymer. IEC affects the proton conductivity significantly. The proton conductivity increases with increasing IEC due to high charge density inside the membrane. [18,24,28] The IEC values of the prepared membranes are presented in Table 3.4.5.1. According to the results of experiments, IEC values increase with the increasing of PAMPS content (i.e. SO_3^{-1}) group in the membrane. The highest IEC value is 1.52 mmol/g that is acquired with 55 PVA: 40 PAMPS: 5 ZIF-8. The membrane in this composition has a higher IEC value as compared to Nafion with 0,97.[34]

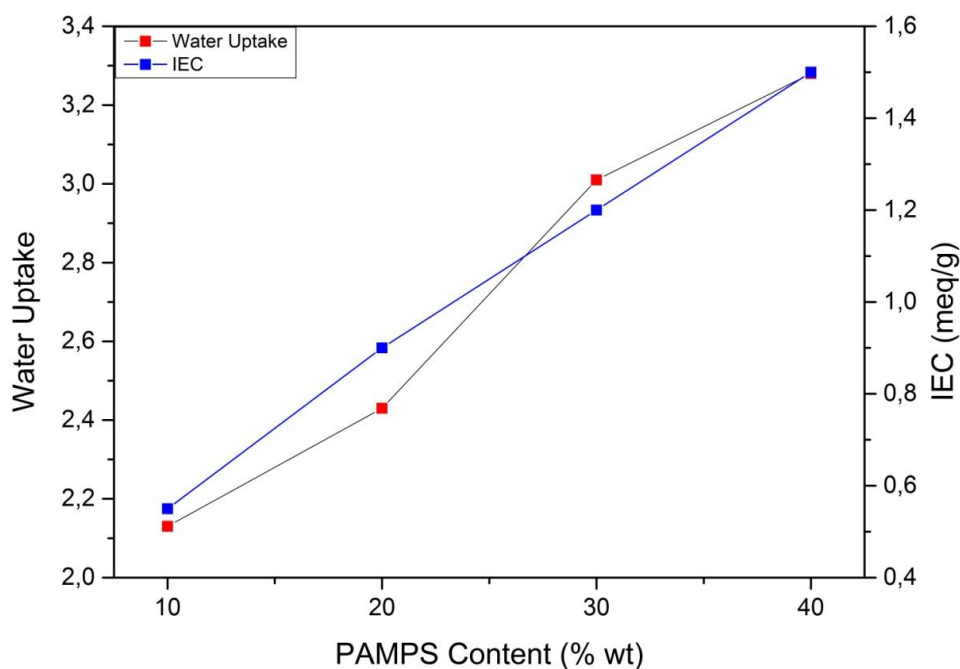


Figure 3.4.5.1 Water uptake and IEC values of the membrane as a function of PAMPS content (%wt)

Fig. 3.4.5.1 shows the both WU and IEC values of the prepared membrane graph as a function of PAMPS content. From this figure it can be seen that both WU and IEC values increase with increasing of PAMPS content in the membrane. As a result of chemical cross-linking of PVA, the hydrophilic hydroxyl groups (-OH) in the PVA react with aldehyde groups (-CHO) in the GA. Therefore, the WU character of the membranes strongly depends on the hydrophilic sulfonic acid groups in PAMPS. [36] Additionally, sulfonic acid groups is the only ion exchangeable groups in the membrane, so the change in IEC values are directly linked to PAMPS content in the membrane. The both WU and IEC values are broadly consistent with similar studies in the literature. As well, the both reached values for WU and IEC are considerably higher than Nafion-117 data in the literature. [34]

3.4.6 Proton Conductivity

Fig. 3.4.6.1 presents the Arrhenius plot of the proton conductivity for the fully hydrated composite membranes. It shows that there is linear temperature dependence between 20 and 80 °C. Notwithstanding the compositions of the membranes, proton conductivities of the membranes enhance with the rising of temperature. As expected, the proton conductivity of the membranes increases with the increasing PAMPS content, as well. For instance, the whereas conductivity of 85PVA:10PAMPS:5ZIF-8 reached 0.001 S cm^{-1} at 80 °C, the conductivity of 55PVA:40PAMPS:5ZIF-8 reached 0.134 S cm^{-1} at 80 °C, thirteen times higher than 85PVA:10PAMPS:5ZIF-8. (Table 3.4.5.1) For comparison purposes, the proton conductivity values for fully hydrated Nafion - 117 are between $0.09 - 0.1 \text{ S cm}^{-1}$ in the literature. [34,35, 41,51] On the other hand, in comparison to 60PVA/40PAMPS, the membrane with 55PVA/40PAMPS/5ZIF-8 has considerably higher proton conductivity values. It may concluded from this, ZIF-8 nanoparticles in the membrane contributes the migration of protons. In that case, the hydrogen atoms on the outer surfaces of ZIF-8 nanoparticles contributed to the proton conduction pathway by making hydrogen bonding network with polymer electrolyte. As well, the defect sites inside the ZIF-8 also aid to proton transfer providing hydrogen bonding.

The activation energies which are derived from the Arrhenius plot of the composite membrane are in between 10.81 and 15.23 kJ mol^{-1} . These results are similar to the activation energy of Nafion-117 for which was reported at 12 kJ mol^{-1} . [41,51] According to these results, the proton migration across the membrane comes about by three mechanism. The first is Grotthuss mechanism in which proton migration from one site to another is controlled by the formation and breaking of hydrogen bonds between a hydroxyl groups or water molecules. In the composite membrane, the number of sulfonic acid groups assist for the Grotthuss mechanism. In the second, the vehicle-type mechanism, a proton combines with solvent molecules in the medium, producing a complex and then diffuses. For instance, a proton combined with water molecule in the medium can migrate by hydronium ion (H_3O^+) through the channels of PVA

polymeric domains. And the third one, protons are transferred inside the membrane along the hydrogen bonding path by generated ZIF-8 nanoparticles.

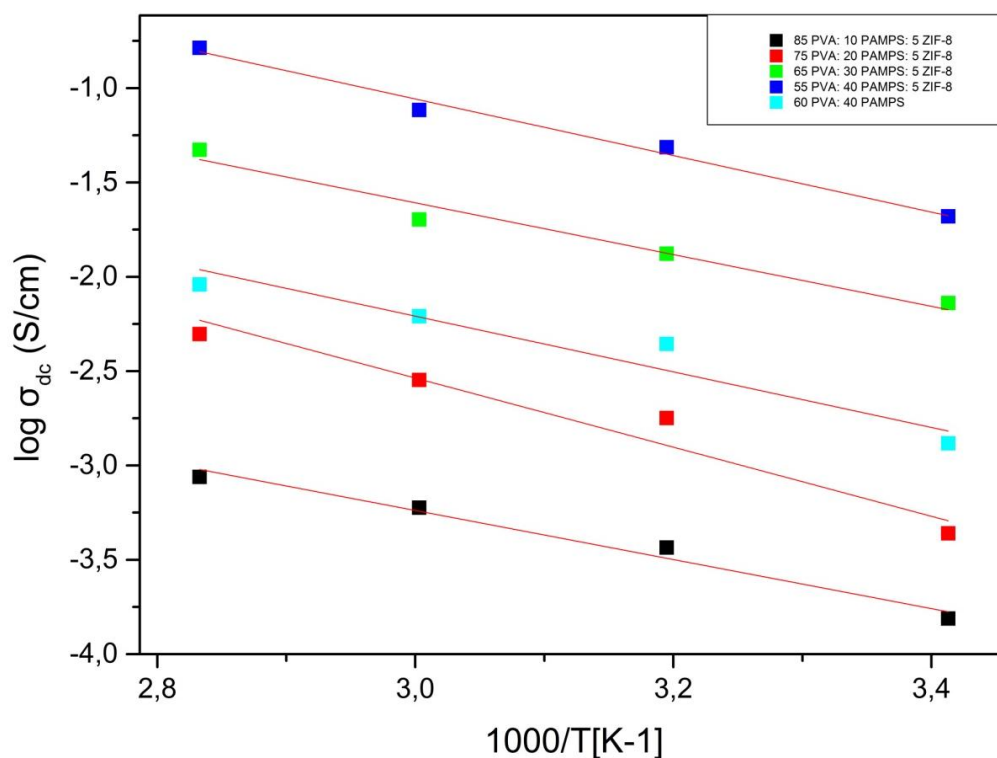


Figure 3.4.6.1 Arrhenius plot for the proton conductivity of composite membranes

3.5 Conclusions

This study reports the preparation of a series of PVA:PAMPS:ZIF-8 proton conducting ternary composite membranes. The findings of our research are quite convincing, and thus the following conclusions can be drawn: SEM and EDX micrograph confirm that all materials uniformly distribute in the membrane. FT-IR spectra confirm the achievement of chemical cross-linking of PVA by GA and also showed that intermolecular interaction between the constituents. Thermal degradation result indicate that the composite membrane can be utilized up to 200 °C. Water uptake (WU) and ion exchange capacity (IEC) tests showed that both values directly link to the PAMPS content in the

membrane and reached values are higher than values of Nafion for the same conditions in the literature. Among the membranes, the fully hydrated membrane with 55PVA:40PAMPS:5ZIF-8 composition showed the best proton conductivity of 0.134 S cm^{-1} at $80 \text{ }^{\circ}\text{C}$ which is comparable to commercially Nafion -117. As well as, it is evident that this study has shown the enhanced effects of ZIF-8 nanoparticles on proton conductivity.

Chapter4

Proton Conducting ZIF-8/PBI Mixed Matrix Membranes For High Temperatures Proton Exchange Membranes Fuel Cells

4.1 Literature Survey

Due to the low operation temperatures, usually at 80 °C, several problems emerge during the operation conditions in a fuel cell. The major challenges for proton exchange membrane fuel cells (PEMFCs) are as follows: (i) low electrode performance because of the slow reduction kinetics of oxygen reduction, (ii) low tolerance to fuel impurities (e.g. CO), (iii) needed of complex water and thermal management system, (iv) low system efficiency due to recovery limited value of the heat. The high temperature proton exchange fuel cells (HTPEMFCs) are a promising technology which can prevail over these challenges. The high temperature correspond to an operation temperature ranging from 100 to 200 °C. HTPEMFCs have been regarded as the reasonable alternative to fuel cells' previously mentioned challenges. Because of the high operation temperature, HTPEMFCs need to different materials for especially electrode and other parts of the device. [66,68,70]

Up to now, great efforts have been made to develop novel proton exchange membrane which operates in anhydrous conditions with high proton conductivity. One of the most effective methods among them relies on the preparation of the acid-base complexes. The backbones of the polymers, which

are used in such a complex, react with acids. In such a reaction, the polymer's backbone acts as a proton acceptor and this results in an ion pair formation. A large body of research has been published on poly(vinylpyrrolidone) (PVP), poly(ether ether ketone) (SPEEK), polyethyleneoxide (PEO), polyethyleneimine (PEI). [68] Several studies have revealed that using amphoteric acid, which can act as an acid and as a base, enhances the proton conductivity of the membrane. And these dual behaviors result in dynamic hydrogen bond forming and breaking. The typical amphoteric acids used in such studies are phosphoric or phosphonic acids. [64-65] However this kind of polymer-acid structures have had some limitations and drawbacks in several ways. For instance, most of the structures in the literature have proton conductivity less than $10^{-3} \text{ S cm}^{-1}$ [73]. On the other hand, excessive acid contents in the polymer causes the gel-like formation, so membrane could not cast.

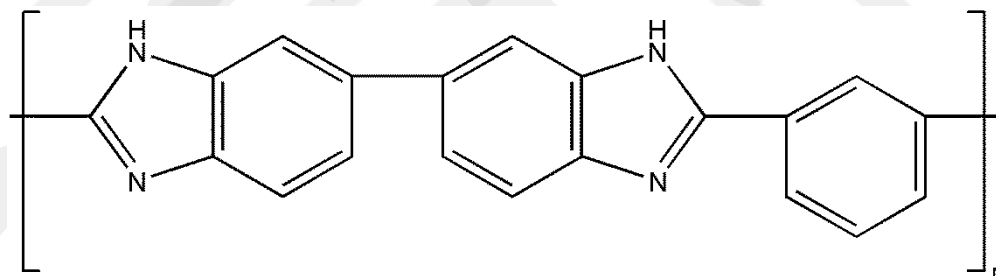


Figure 4.1.1 The chemical structure of poly[2,2'-(m-phenylene)-5,5'-bisbenzimidazole]

Polybenzimidazole (PBI) is a basic heterocyclic polymer with outstanding mechanical and thermal stability. Actually, PBI stands for two different meanings. While PBI alludes to the general name of the aromatic heterocyclic polymer embodying benzimidazole units, it also specifies the commercial product under the trademark Celazole®. (Fig. 4.1.1) The first example of the phosphoric acid doped PBI used as fuel cell membrane is presented in [Savinelli]The results obtained by Savinelli demonstrate that when PBI is doped by aqueous phosphoric acid, PBI/H₃PO₄ acid-base complex exhibit high proton conductivity at high temperatures. From that time, a considerable amount of

literature, which are related to the increase of proton conductivity of PBI/H₃PO₄, improvement of thermal and mechanical properties of the complex and enhancement of the operation parameters, have been published on PBI/H₃PO₄ membrane system. These studies generally include incorporation of inorganic and organic additives into PBI/H₃PO₄ complex [65,66], blending of PBI with different polymers [69], synthesizing of different PBI by monomer modifications [73]. More recent studies have discovered the possibility that nanoporous PBI filled with H₃PO₄ could considerably enhance the proton conductivity of the membrane. Pina et al. [72] studied mesoporous PBI (mp-PBI) and showed that mp-PBI doped with excess H₃PO₄ exhibits higher proton conductivity than non-porous PBI doped with excess H₃PO₄. The major drawback of this approach is the complexity in synthesizing of mp-PBI. To overcome this obstacle, the composite membrane which consist of PBI and nanoporous material could be a good option. However, to the author's best knowledge, very few publications can be found available in the literature that discusses PBI/nanoporous additive mixed matrix membranes (MMMs). When the polymer host is filled by the conventional filler materials such as zeolites, silica, face compatibility problems occur between the host-filler interfaces because of the inorganic nature of the traditional fillers materials.

MOFs -metal organic frameworks - ,which are a new class of ordered porous materials, consist of inorganic metal clusters and organic linkers. (47-48.) Since they could be designed for the desire function by tailoring, MOFs attract much attention from diverse research disciplines. Compared with other porous materials (e.g. zeolites), MOFs has higher porosity. Thanks to organic linkers in the MOFs structure, they will not produce the interface incompatibilities of traditional fillers when they are used as fillers in the MMMs. Current research on PBI/MOFs is mainly focused on gas separation. [60-63]

However, there has been relatively little literature published on proton conducting polymer/MOF membrane. Liang et al. [67] reported the proton conducting 2D MOF/PVP under relatively low humidity. Xu et al.[49] studied

oriented MOF/ polymer electrospun nano-composite membranes and showed that proton conductivity values for this composite structures is about 10^{-2} S cm⁻¹ at 160 °C under anhydrous condition.

Herein, we present a proton conducting MMM composite membrane, which consists of ZIF-8 and PBI. While PBI [poly[2,2'-(m-phenylene)-5,5'-bisbenzimidazole]], is used as host polymer, the ZIF-8 is used as filler in this study. Zeolitic Imidazolate Frameworks (ZIFs) are a sub-class of MOFs which are akin to pore topologies with zeolites and show superior chemical and thermal stability. ZIF-8 consists of Zn (II) metal cation linking with 2-methylimidazolate (Hmim) anion in the tetrahedral framework that forms the sodalite (SOD) zeolite structure with large cavities (11.6 Å) and small pore size (3.4 Å). As a result of Hmim linkers, ZIF-8 is vastly hydrophobic that provides a high water stability for the framework when exposed to water. Thanks to its hydrophobic nature and better compatibility with polymer matrix, ZIF-8 is anticipated to improve water management of the membrane. Moreover, the linker 2-methylimidazolate (Hmim) has a similar molecular structure that of imidazole and pyrazole, ZIF-8 can assist for the proton conduction by the similar mechanism as imidazole and pyrazole [49,52,57].

4.2 Experimental

4.2.1 Materials

2-Methylimidazole (Hmim with 97% purity), Zinc Nitrate Hexahydrate (Zn (NO₃)₂·6H₂O, 99% purity – metal based), 1-Methyl-2-pyrrolidinone (NMP, 99+%) were both purchased from Alfa Aesar. Polybenzimidazole (PBI, 1.1 IV Powder) was purchased from PBI Performance Products, Inc. Methanol with 99.9 % purity and ortho-phosphoric acid (85%) were purchased from Merck.

4.2.2 Synthesis of ZIF-8 Nanoparticles

In the synthesis of the ZIF-8 nanoparticles, the same procedure was followed which is described by Cravillion et al. [45] Shortly, 1.0510 g (3.53 mmol) $\text{Zn}(\text{NO}_3)_2 \cdot 6\text{H}_2\text{O}$ was dissolved in 50 ml methanol and 2.3353 g (28.3 mmol) Hmim was dissolved in 50 ml methanol. Then first solution was poured into second solution. And the final solution was vigorously stirred room temperature for 1 h. At the end of the stirring process, the milky solution was centrifugated at 7500 rpm two times and nanoparticles were washed by methanol. The yield of ZIF-8 was ~30 % based on Zn. Afterward; some were heated in the vacuum oven at 80 °C during 24 h for further characterization. The rest of nanoparticles were kept in methanol during all next steps. The yield of ZIF-8 was ~30 % based on Zn.

4.2.3 Membrane Preparation

In the synthesis of the PBI/ZIF-8 nano-composite membranes, the following procedures in literature were followed. [62] Firstly, PBI grains were dissolved in NMP at 120 C by vigorously stirring for 48 h. The concentration of the PBI/NMP solution is 1.5 wt %. And then, the prepared solution was filtered via using 1 μm PTFE syringe filters. ZIF-8 nanoparticles in methanol were re-dispersed in NMP at room temperature. To obtain well dispersed suspension, ZIF-8/NMP was stirred and sonicated periodically. After that, certain amounts of ZIF-8/NMP suspension was added to certain amounts of PBI/NMP solution. The final mixtures were stirred vigorously for overnight. The well dispersed PBI/ZIF-8/NMP solutions were cast into glasses petri dishes. The casting membranes were put in hood under ventilation during the overnight. Finally, casting membranes were put into vacuum oven at 70 °C for 12 h. And then, the membranes were peeled off from the glass petri dishes and put into vacuum oven at 200 °C for 12 h to evaporate the residual solvent. Finally, a solvent exchange method was applied to take out the residual solvent inside the ZIF-8 pores. Accordingly, all of the membranes were kept in methanol at the room

temperature for 48 h. And then, to evaporate the methanol, the membranes were dried in a vacuum oven at 200 °C. The final concentration of the ZIF-8 to all membrane was varied at 0, 12.5, 25, 37.5, 50 wt %. The thickness of the prepared membranes are in between 50-80 μm.

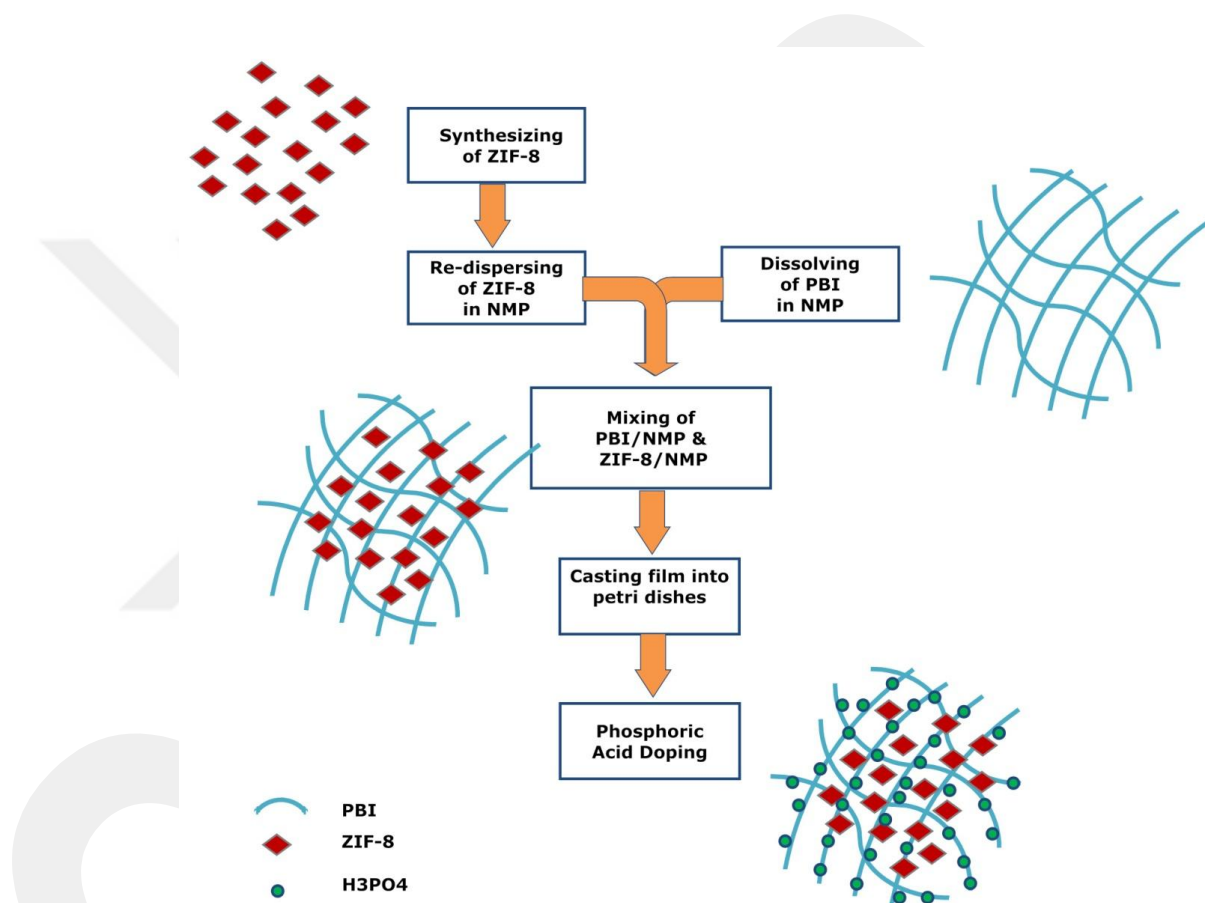


Figure 4.2.3.1 Scheme for preparation steps of mixed matrix membranes

4.2.4 Phosphoric acid doping

All prepared membranes were doped with ortho-phosphoric acid for expected proton conductivity. The following procedure was followed in the doping process. Concordantly, all PBI membranes were immersed in 14 M ortho-phosphoric at 80 °C for 24 h. And then all the membranes were cooled

down to room temperature and wiped with the tissue paper to remove the excess acid on the surface of the membranes. In the next step, all the membranes were put in a vacuum oven and were dried at 120 C for overnight. The phosphoric acid doping level of the membranes were calculated according to the following equation:

$$\lambda = \frac{(W_d - W_0)}{W_0} \quad (4.2.4.1)$$

where W_d and W_0 , are the weight of dried membrane after doping, and the weight of dried membrane before doping, respectively.



Figure 4.2.4.1 Photo of acid doped mixed matrix membrane

4.3 Characterization

4.3.1 X-Ray Diffraction (XRD)

X-ray diffraction pattern of the prepared membranes were acquired by using Bruker AXS D8 Advance. The diffraction angle (2θ) ranging from 50 to 400 was scanned at a scan rate 0.010 min^{-1} with 1.54 nm wavelength radiation which is generated by $\text{CuK}\alpha$.

4.3.2 Fourier Transform Infrared Spectroscopy (FT-IR)

The prepared membrane was examined by using Attenuated Total Reflectance Fourier Transform Spectroscopy (ATR-FTIR) on Thermo Nicolet 6700. Spectrum was obtained with 4 cm^{-1} resolution between $400 - 4000 \text{ cm}^{-1}$.

4.3.3 Scanning Electron Microscopy (SEM)

The morphologies of the prepared membranes were examined by Zeiss EVO LS 10. To affirm the existence and homogenous distributions of the ZIF-8 nanoparticles in the composite membrane.

4.3.4 Proton Conductivity

Proton conductivity measurements of the prepared membranes were performed via using a Novocontrol dielectric-impedance analyzer. The films were sandwiched between platinum blocking electrodes and the conductivity was measured in the frequency range from 1 Hz to 3 MHz as a function of temperature, which was varied from $20 \text{ }^{\circ}\text{C}$ to $160 \text{ }^{\circ}\text{C}$ in $20 \text{ }^{\circ}\text{C}$ intervals.

4.4 Results & Discussions

4.4.1 X-Ray Diffraction (XRD)

The XRD pattern of all MMMs and ZIF-8 are given in Fig. 4.4.1.1. The XRD pattern of the synthesized ZIF-8 nano-crystals are well matched to the ZIF-8 XRD pattern in the literature. [45] As can be seen from Fig. 4.4.1.1 there are some peaks which deal with the ZIF-8 nanoparticles on the XRD patterns of the membranes. This result indicates that even after being mixed with PBI host polymer and being doped with H_3PO_4 , crystal structure of the ZIF-8 remains unchanged. Additionally, When the ZIF-8 loading increases from 12.5 wt% to 50 wt%, intensities of the ZIF-8 peaks become stronger and the amorphous peak of the PBI diminishes.

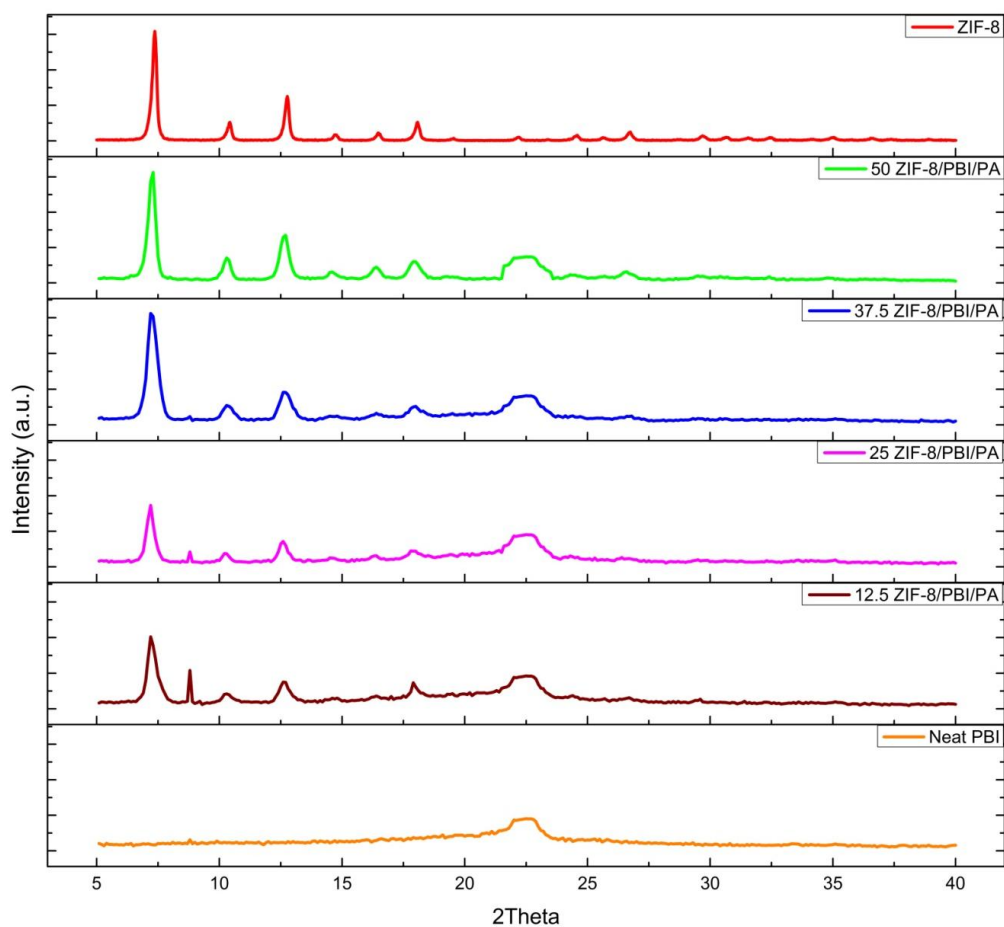


Figure 4.4.1.1 XRD pattern of ZIF-8 and mixed matrix membranes

4.4.2 Fourier Transform Infrared Spectroscopy (FT-IR)

ATR/FT-IR was used in order to present intermolecular and/or interchain hydrogen bonding between host polymers and ZIF-8 nanoparticles. Transmittance FT-IR spectra of the neat PBI membrane and ZIF-8/PBI mixed matrix membranes are shown in Fig X. The broad absorption peaks occurred in all spectra at around 3300 cm^{-1} are assigned to N-H stretching. The peaks at around 1660 cm^{-1} are originated from C=C in between imidazole and benzene ring. While the peaks at around 1100 cm^{-1} are assigned to stretching of C-C. And the peaks at around 800 and 692 cm^{-1} are raised from C-H out of plane bending of aromatic hydrogen atoms. [57,62,63] From this figure it can be seen that adding of ZIF-8 into PBI host causes the decrease in the intensity of peaks. This finding has implication for a strong interaction between ZIF-8 and PBI.

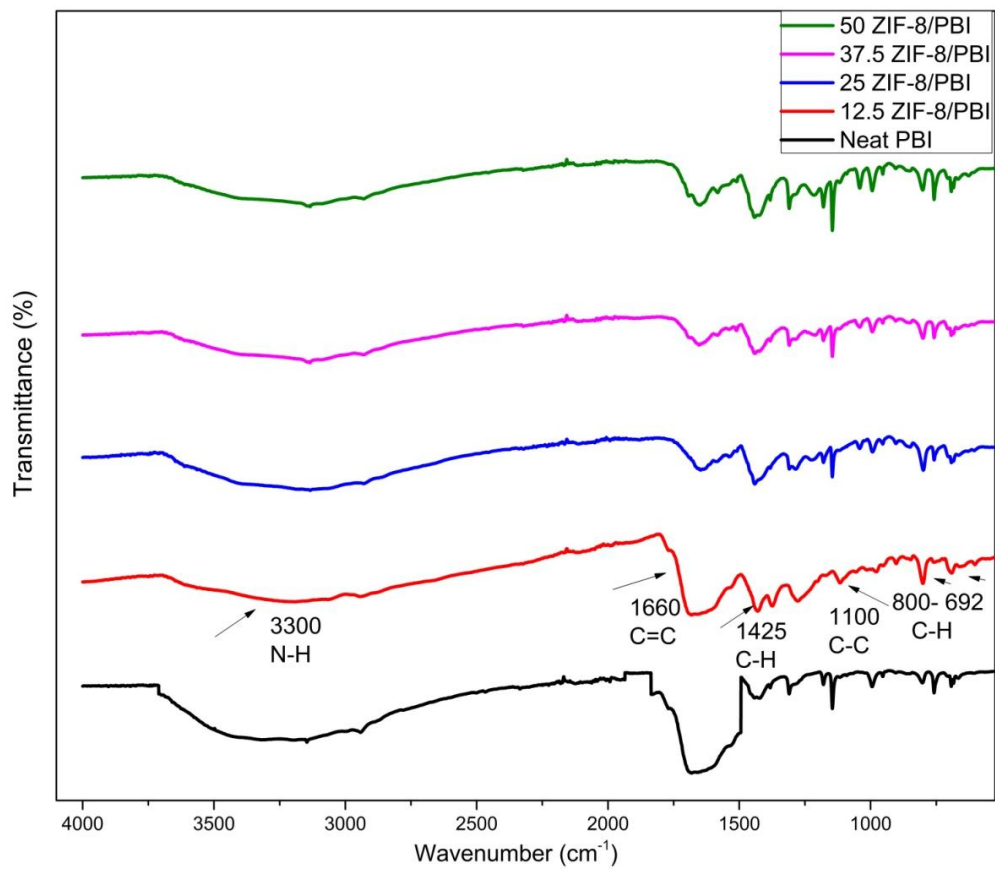


Figure 4.4.2.1 FT-IR spectra of mixed matrix membranes

4.4.3 Scanning Electron Microscopy (SEM)

SEM analysis was performed to examine the morphology of ZIF-8/PBI mixed matrix membranes and interfaces compatibility between ZIF-8 and PBI. The top-surface and cross-sectional SEM micrographs of the 12.5 ZIF-8/PBI are represented in Fig. 4.4.3.1 As can be seen from Fig. 4.4.3.1(a), the top surface of the membrane is uneven due to the existence of ZIF-8 nanoparticles. As shown in Fig. 4.4.3.2(b), the cross-sectional surface of the membrane has no void and it can be seen that there are no incompatibilities between ZIF-8 and PBI phases. This finding indicates that ZIF-8 and PBI are mixed very well. Also, the thickness of the membrane is measured as about 84 μm .

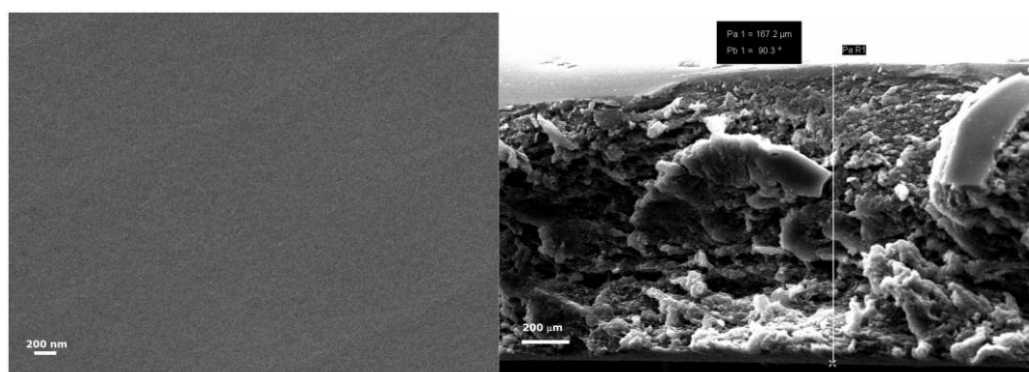


Figure 4.4.3.1 SEM micrograph MMM with 12.5 ZIF-8/PBI composition: (a) Surface morphology (magnification 100 000×), (b) Cross-section morphology (magnification 2500 ×)

4.4.4 Proton Conductivity

Temperature dependence of proton conductivity for anhydrous state neat PBI/PA and ZIF-8/PBI/PA composite membranes is presented Fig. 4.4.1.1. As can be seen from Fig. 4.4.1.1, all of the membrane showed proton conductivity. Because of its special proton conduction ability via self-ionization and self-dehydration, the proton conductivity of the 100 % PA is about 0.025 S cm^{-1} . [70] On the other hand, addition of water into the 100 % PA causes an increase in the number of charge carriers because of dissociation. However, the acid-doped PBI is in a solid phase, hence the principal effect on proton conductivity comes from the solid PBI phase. In the case of neat PBI, proton transfer over the N-sites is theoretically possible by the Grotthuss mechanism and reported values in the literature support this theory. [71] Instead, in PA-doped PBI membrane, a phosphoric acid molecule is immobilized by protonating a benzimidazole ring. [71] According to the literature, the proton conduction in acid-doped PBI membrane is mainly controlled by the Grotthuss mechanism. [68]

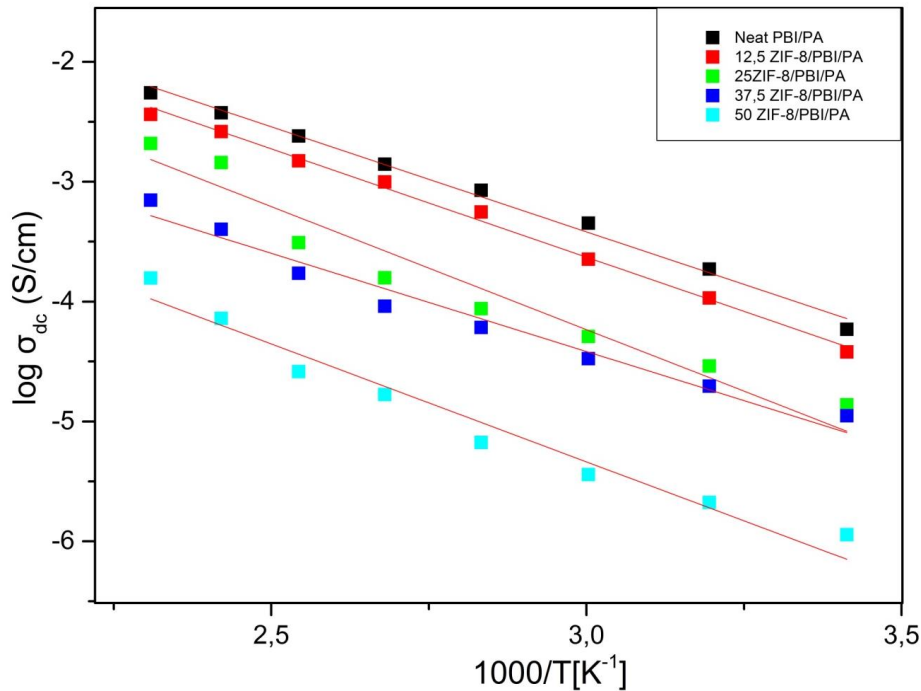


Figure 4.4.1.1 Arrhenius plot of MMM membranes

The proton conductivity for all membrane increases with increasing of temperature. The membrane with 12.5ZIF-8/PBI composition is showed proton conductivity about 0.045 S cm^{-1} at $160 \text{ }^{\circ}\text{C}$. However, the proton conductivity value of the pristine PBI is about 0.07 S cm^{-1} . Though PA doping level of the membrane with 12.5ZIF-8/PBI composition is higher than the value for pristine PBI, the proton conductivity of 12.5ZIF-8/PBI is about half of pristine PBI.(Table 4.4.1.1) This result indicate that the stored PA molecules in the pores of ZIF-8 nanoparticles do not contribute the proton migration. Beside, the increasing in ZIF-8 content in the membrane causes decreasing the PA doping level of the membrane. The reason is that, hydrophobic nature of the ZIF-8 nanoparticles is hindered the diffusion of the PA molecules by assisting of water.

Specimen	Slope	Act. E. (e.V)	Act. E. (kJ/mol)	PA Doping Level	P. Conductivity (S/cm)
Neat PBI/PA	-1.75315	0.15	14.57	3.88	0.0075
12,5 ZIF-8/PBI/PA	-1.80755	0.17	16.36	4.30	0.0045
25 ZIF-8/PBI/PA	-2.05311	0.18	17.07	3,67	0.0026
37,5 ZIF-8/PBI/PA	-1.63941	0.14	13.63	3,27	0.0014
50 ZIF-8/PBI/PA	-1.96798	0.16	15.02	2,84	0.0006

Table 4.4.3.1 Physicochemical properties of mixed matrix membranes

4.5 Conclusions

This study reports the preparation of a series of ZIF-8/PBI proton conducting mixed matrix membranes. The findings of our research are quite convincing, and thus the following conclusions can be drawn: SEM micrograph confirm that all materials uniformly distribute in the membrane. FT-IR spectra confirm intermolecular interaction between the constituents. Among the membranes, the membrane with 12.5ZIF-8/PBI composition showed the highest proton conductivity of 0.045 S cm^{-1} at $160 \text{ }^{\circ}\text{C}$ in anhydrous medium which is comparable to PBI .

Chapter 5

Conclusions

In this thesis, mechanical robust, thermally stable high proton conducting composite membranes were prepared. To the best of our knowledge, the ZIF-8 nanoparticles were used as a filler material in the composite membrane for the first time for the proton exchange membrane applications. The study in this thesis showed that the presence of the ZIF-8 nanoparticles in the membrane does not cause any inter-phase incompatibility. Besides, by forming hydrogen bonding, they assist in proton transfer in the membrane. The findings suggest that the applied method in this thesis could also be useful for preparing similar composite membranes. The findings are of direct practical relevance.

In our future research we intend to concentrate on proton conducting MOF and proton conducting MOF/polymer composite membranes any more. After publishing the obtained results here, the next stage of our research will be preparing ZIF-8/different host polymer.

BIBLIOGRAPHY

- [1] F. Barbir, "PEM Fuel Cells Theory and Practice" Academic Press (2012).
- [2] C. Spiegel "PEM Fuel Cells Modeling and Simulation Using MATLAB[®]" Academic Press (2008).
- [3] David P. Wilkinson, Jiujun Zhang, Rob Hui, Jeffrey Fergus, Xianguo Li Proton Exchange Membrane Fuel Cells- Materials Properties and Performance (Green Chemistry and Chemical Engineering), CRC Press (2009)
- [4] Bagotsky V.S. Fuel cells- Problems and solutions, Wiley (2009)
- [5] 2014 Key World Energy Statistics, International Energy Agency (IEA)
- [6] <http://www.globalcarbonproject.org/> (last access: 29.06.2015)
- [7] Tracking Clean Energy Progress 2014, International Energy Agency (IEA), 2014
- [8] <http://www.worldcoal.org/coal/uses-of-coal/coal-electricity/> (last access: 29.06.2015)
- [9] <http://energy.gov/eere/fuelcells/comparison-fuel-cell-technologies> (last access: 29.06.2015)
- [10] <http://www.doitpoms.ac.uk/tlplib/fuel-cells/> (last access: 29.06.2015)
- [11] Jiujun Zhang PEM Fuel Cell Electrocatalysts and Catalyst Layers, Springer, (2008)
- [12] S. Litster, G. McLean (2004), " PEM fuel cell electrodes", Journal of Power Sources 130 61–76
- [13] Yun Wang, Ken S. Chen, Jeffrey Mishler ,Sung Chan Cho, Xavier Cordobes Adroher (2011), Applied Energy 88 , 981–1007
- [14] Li, Q., R. He, et al. (2004). "PBI-Based Polymer Membranes for High Temperature Fuel Cells - Preparation, Characterization and Fuel Cell Demonstration." Fuel Cells 4(3): 147-159.

[15] Han Gao and Keryn Lian, (2014) " Proton-conducting polymer electrolytes and their applications in solid supercapacitors: a review", RSC Adv., 2014,4, 33091-33113

[16] Klaus-Dieter Kreuer, (1996), Proton Conductivity: Materials and Applications, Chem. Mater. 8, 610-641

[17] Anis, A., S. M. Al-Zahrani, et al. (2011). "Fabrication and Characterization of Novel Crosslinked Composite Membranes for Direct Methanol Fuel Cell Application - Part II. Poly (Vinyl Alcohol-Co-Vinyl Acetate-Co-Itaconic Acid)/Silicotungstic Acid Based Membranes." International Journal of Electrochemical Science 6(7): 2652-2671.

[18] Chen, X. X. and G. B. Guo (2012). "Studies on preparation and properties of SiO₂/PVA-PAMPS composite Membrane." Renewable and Sustainable Energy li, Pts 1-4 512-515: 2007-2010.

[19] Chikh, L., V. Delhorbe, et al. (2011). "(Semi-)Interpenetrating polymer networks as fuel cell membranes." Journal of Membrane Science 368(1-2): 1-17.

[20] Dai, C. A., C. J. Chang, et al. (2009). "Polymer actuator based on PVA/PAMPS ionic membrane: Optimization of ionic transport properties." Sensors and Actuators a-Physical 155(1): 152-162.

[21] Dai, C. A., C. C. Hsiao, et al. (2009). "A membrane actuator based on an ionic polymer network and carbon nanotubes: the synergy of ionic transport and mechanical properties." Smart Materials & Structures 18(8).

[22] Feng, X., L. Chen, et al. (2008). "POLY 473-Preparation of PAMPS/PVA electrosensitive hydrogel fibers." Abstracts of Papers of the American Chemical Society 235.

[23] Hamaya, T., S. Inoue, et al. (2006). "Novel proton-conducting polymer electrolyte membranes based on PVA/PAMPS/PEG400 blend." Journal of Power Sources 156(2): 311-314.

[24] Higa, M., S. Y. Feng, et al. (2015). "Characteristics and direct methanol fuel cell performance of polymer electrolyte membranes prepared from poly(vinyl alcohol-b-styrene sulfonic acid)." Electrochimica Acta 153: 83-89.

[25] Higa, M., M. Sugita, et al. (2010). "Poly(vinyl alcohol)-based polymer electrolyte membranes for direct methanol fuel cells." Electrochimica Acta 55(4): 1445-1449.

[26]Jiang, G. P., J. Zhang, et al. (2015). "Bacterial nanocellulose/Nafion composite membranes for low temperature polymer electrolyte fuel cells." *Journal of Power Sources* 273: 697-706.

[27]Jung, K. H., B. Pourdeyhimi, et al. (2011). "Synthesis and Characterization of Polymer-Filled Nonwoven Membranes." *Journal of Applied Polymer Science* 119(5): 2568-2575.

[28]Kumar, G. G., P. Uthirakumar, et al. (2009). "Fabrication and electro chemical properties of poly vinyl alcohol/para toluene sulfonic acid membranes for the applications of DMFC." *Solid State Ionics* 180(2-3): 282-287

[29]Kuzume, A., Y. Miki, et al. (2013). "Characterisation of PAMPS-PSS pore-filling membrane for direct methanol fuel cell." *Journal of Membrane Science* 446: 92-98.

[30]Lin, S. B., C. H. Yuan, et al. (2013). "Electrical Sensitivity and Mechanical Properties of Fast Responsive PAMPS-PAA-PVA T-IPN Hydrogels." *Advances in Polymer Technology* 32: E20-E31.

[31]Liu, C. P., C. A. Dai, et al. (2014). "Novel proton exchange membrane based on crosslinked poly(vinyl alcohol) for direct methanol fuel cells." *Journal of Power Sources* 249: 285-298.

[32]Qiao, J., S. Ikesaka, et al. (2007). "Life test of DMFC using poly(ethylene glycol) bis(carboxymethyl) ether plasticized PVA/PAMPS proton-conducting semi-IPNs." *Electrochemistry Communications* 9(8): 1945-1950.

[33]Qiao, J., S. Ikesaka, et al. (2007). "New binders for MEA fabrication for low temperature DMFCs using PVA-PAMPS proton-conducting semi-IPN membranes." *Electrochemistry* 75(2): 126-129.

[34]Qiao, J. L., T. Hamaya, et al. (2005). "Chemically modified poly(vinyl alcohol)-poly(2-acrylamido-2-methyl-1-propanesulfonic acid) as a novel proton-conducting fuel cell membrane." *Chemistry of Materials* 17(9): 2413-2421.

[35]Qiao, J. L., T. Hamaya, et al. (2005). "New highly proton conductive polymer membranes poly(vinyl alcohol)-2-acrylamido-2-methyl-1-propanesulfonic acid (PVA-PAMPS)." *Journal of Materials Chemistry* 15(41): 4414-4423.

[36]Qiao, J. L., T. Hamaya, et al. (2005). "New highly proton-conducting membrane poly(vinylpyrrolidone)(PVP) modified poly(vinyl alcohol)/2-acrylamido-2-methyl-1-propanesulfonic acid (PVA-PAMPS) for low temperature direct methanol fuel cells (DMFCs)." *Polymer* 46(24): 10809-10816.

[37]Qiao, J. L. and T. Okada (2006). "Highly durable, proton-conducting semi-interpenetrating polymer networks from PVA/PAMPS composites by incorporating plasticizer variants." *Electrochemical and Solid State Letters* 9(8): A379-A381.

[38]Qiao, J. L. and T. Okada (2007). "PVA-PAMPS based semi-IPNs as new type of proton-conducting membranes for low-temperature DMFC." *Journal of New Materials for Electrochemical Systems* 10(4): 231-236.

[39]Qiao, J. L., T. Okada, et al. (2009). "High molecular weight PVA-modified PVA/PAMPS proton-conducting membranes with increased stability and their application in DMFCs." *Solid State Ionics* 180(23-25): 1318-1323.

[40]Salarizadeh, P., M. Javanbakht, et al. (2013). "Preparation, characterization and properties of proton exchange nanocomposite membranes based on poly(vinyl alcohol) and poly(sulfonic acid)-grafted silica nanoparticles." *International Journal of Hydrogen Energy* 38(13): 5473-5479.

[41]Yang, C. C., S. J. Lue, et al. (2011). "A novel organic/inorganic polymer membrane based on poly(vinyl alcohol)/poly(2-acrylamido-2-methyl-1-propanesulfonic acid/3-glycidyloxypropyl trimethoxysilane polymer electrolyte membrane for direct methanol fuel cells." *Journal of Power Sources* 196(10): 4458-4467.

[42]Yuan, C. H., G. B. Guo, et al. (2012). "The influence on proton conductivity and methanol permeability of SiO₂/PVA-PAMPS composite Membrane." *Frontiers of Manufacturing Science and Measuring Technology* Ii, Pts 1 and 2 503-504: 625-628.

[43]Yuan, C. H., S. B. Lin, et al. (2009). "Preparation and Property Characterization of Macroporous PAMPS/PVA S-IPN Hydrogels." *Acta Chimica Sinica* 67(16): 1929-1935.

[44]Amirilargani, M. and B. Sadatnia (2014). "Poly(vinyl alcohol)/zeolitic imidazolate frameworks (ZIF-8) mixed matrix membranes for pervaporation dehydration of isopropanol." *Journal of Membrane Science* 469: 1-10.

[45]Cravillon, J., R. Nayuk, et al. (2011). "Controlling Zeolitic Imidazolate Framework Nano- and Microcrystal Formation: Insight into Crystal Growth by Time-Resolved In Situ Static Light Scattering." *Chemistry of Materials* 23(8): 2130-2141.

[46] K. S. Park, Z. Ni, A. P. Côté, J. Y. Choi, R. D. Huang, F. J. Uribe-Romo, H. K. Chae, M. O'Keeffe, O. M. Yaghi, (2006) "Exceptional Chemical and Thermal Stability of Zeolitic Imidazolate Frameworks", *Proc. Natl. Acad. Sci. U.S.A.*, 2006, 103, 10186-10191.

- [47] J. L. C. Rowsell, O. M. Yaghi, (2004) "Metal-Organic Frameworks: A New Class of Porous Materials" *Microporous Mesoporous Mater.*, 2004, 73, 3-14.
- [48] H. Furukawa, K. E. Cordova, M. O'Keeffe, O. M. Yaghi, (2013) "The Chemistry and Applications of Metal-Organic Frameworks" *Science*, 2013, 341, 1230444.
- [49] Bin Wu , Jiefeng Pan , Liang Ge , Liang Wu , Huanting Wang, Tongwen Xu (2014), "Oriented MOF-polymer Composite Nanofiber Membranes for High Proton Conductivity at High Temperature and Anhydrous Condition
- [50] Paula Barbosa, Nataly C. Rosero-Navarro, Fa-Nian Shi, Filipe M.L. Figueiredo (2015)"Protonic Conductivity of Nanocrystalline Zeolitic Imidazolate Framework 8" *Electrochimica Acta* 153 19–27
- [51] Yosbitsugu Sonof Per Ekdunge, and Daniel Simonsson, "Proton Conductivity of Nafion 117 as Measured by a Four-Electrode AC Impedance Method" (1996) *J. Electrochem. Soc.*, Vol. 143, No. 4
- [52] Devproshad K. Paul, Richard McCreery, and Kunal Karan (2014) "Proton Transport Property in Supported Nafion Nanofilm Films by Electrochemical Impedance Spectroscopy" *Journal of The Electrochemical Society*, 161 (14) F1395-F1402
- [53] Xuemei Wu, Want Che, Xiaom Yan, Gaohon He , Junjun Wang, Ying Zhang, and Xiaoping Zhu (2014) "Enhancement of hydroxide conductivity by the diquaternization strategy for poly(ether ether ketone) based anion exchange membranes" *J. Mater. Chem. A*, 2, 12222
- [54] Hazel E. Assendert and Alan H. Windle, (1996) "Crystallinity in poly(vinyl alcohol).1. An X-ray diffraction study of atactic PVOH" *POLYMER* Volume 39 Number 18
- [55] Guangshan Zhu et al. (2013)"From metal–organic framework (MOF) to MOF–polymer composite membrane: enhancement of low-humidity proton conductivity", *Chem. Sci.*, 4, 983
- [56] Yun-Sheng Ye, John Rick and Bing-Joe Hwang (2012) "Water Soluble Polymers as Proton Exchange Membranes for Fuel Cells", *Polymers* 2012, 4, 913-963
- [57] Bhaskar, A., R. Banerjee, et al. (2014). "ZIF-8@PBI-Bul composite membranes: elegant effects of PBI structural variations on gas permeation performance." *Journal of Materials Chemistry A* 2(32): 12962-12967.

- [58] Biswal, B. P., A. Bhaskar, et al. (2015). "Selective interfacial synthesis of metal-organic frameworks on a polybenzimidazole hollow fiber membrane for gas separation." *Nanoscale* 7(16): 7291-7298.
- [59] Panapitiya, N. P., S. N. Wijenayake, et al. (2014). "Stabilization of immiscible polymer blends using structure directing metal organic frameworks (MOFs)." *Polymer* 55(8): 2028-2034.
- [60] Shi, G. M., H. M. Chen, et al. (2013). "Sorption, swelling, and free volume of polybenzimidazole (PBI) and PBI/zeolitic imidazolate framework (ZIF-8) nano-composite membranes for pervaporation." *Polymer* 54(2): 774-783.
- [61] Shi, G. M., T. X. Yang, et al. (2012). "Polybenzimidazole (PBI)/zeolitic imidazolate frameworks (ZIF-8) mixed matrix membranes for pervaporation dehydration of alcohols." *Journal of Membrane Science* 415: 577-586.
- [62] Yang, T. and T. S. Chung (2013). "High performance ZIF-8/PBI nano-composite membranes for high temperature hydrogen separation consisting of carbon monoxide and water vapor." *International Journal of Hydrogen Energy* 38(1): 229-239.
- [63] Yang, T. X., G. M. Shi, et al. (2012). "Symmetric and Asymmetric Zeolitic Imidazolate Frameworks (ZIFs)/Polybenzimidazole (PBI) Nanocomposite Membranes for Hydrogen Purification at High Temperatures." *Advanced Energy Materials* 2(11): 1358-1367.
- [64] R. Bouchet , E. Siebert "Proton conduction in acid doped polybenzimidazole *Solid State Ionics*" (1999) 118 287–299
- [65] Ronghuan He, Qingfeng Li, Gang Xiao, Niels J. Bjerrum (2003)"Proton conductivity of phosphoric acid doped polybenzimidazole and its composites with inorganic proton conductors" *Journal of Membrane Science* 226 (2003) 169–184
- [66] Y.-L. Ma, J. S. Wainright, M. H. Litt, and R. F. Savinell, (2004) "Conductivity of PBI Membranes for High-Temperature Polymer Electrolyte Fuel Cells", *Journal of The Electrochemical Society*, 151 ~1 ! A8-A16
- [67] Padmini Ramaswamy, Norman E. Wong and George K. H. Shimizu, (2014), "MOFs as proton conductors – challenges and opportunities" *C h e m . S o c . R e v .* , 2014, 43, 5913
- [68] Waldemar Bujalski et al. (2013) "High temperature (HT) polymer electrolyte membrane fuel cells (PEMFC) - A review" *Journal of Power Sources* 231 264e278

[69] Zicheng Zuo, Yongzhu Fu and Arumugam Manthiram, (2012) "Novel Blend Membranes Based on Acid-Base Interactions for Fuel Cells" *Polymers* 2012, 4, 1627-1644

[70] Robert F. Savinell, Niels J. Bjerrum et al. (2009) "High temperature proton exchange membranes based on polybenzimidazoles for fuel cells" *Progress in Polymer Science* 34 (2009) 449–477

[71] Juan Antonio Asensio, Eduardo M. Sanchez and Pedro Gomez-Romero, (2010), "Proton-conducting membranes based on benzimidazole polymers for high-temperature PEM fuel cells. A chemical quest" *Chem. Soc. Rev.*, 2010, 39, 3210–3239

[72] M.P. Pina et al. (2014), "Nanoporous PBI membranes by track etching for high temperature PEMs" *Journal of Membrane Science* 454) 243–252

[73] Steve Lien-Chung Hsu et al. (2014) "A novel asymmetric polybenzimidazole membrane for high temperature proton exchange membrane fuel cells" *J. Mater. Chem. A*, 2014, 2, 4225

[74] Ronald R. Chance et al. (2013) "Investigating the Intrinsic Ethanol/Water Separation Capability of ZIF-8: An Adsorption and Diffusion Study" *J. Phys. Chem. C* 2013, 117, 7214 –7225

[75] David S. Sholl et al., (2013), "Adsorption and Diffusion of Small Alcohols in Zeolitic Imidazolate Frameworks ZIF-8 and ZIF-90" *J. Phys. Chem. C* 2013, 117, 3169 –3176

[76] Sankar Nair et al., (2013) "Exploring the Framework Hydrophobicity and Flexibility of ZIF-8: from Biofuel Recovery to Hydrocarbon Separations", *J. Phys. Chem. Lett.* 2013, 4, 3618 –3622